fractal and fractional

MDPI

Article

Investigating a Nonlinear Fractional Evolution Control Model Using $\mathbb{W}$-Piecewise Hybrid Derivatives: An Application of a Breast Cancer Model

Hicham Saber [1], Mohammed A. Almalahi [2,3], Hussien Albala [4], Khaled Aldwoah [5,*], Amer Alsulami [6], Kamal Shah [7] and Abdelkader Moumen [1]

[1] Department of Mathematics, College of Science, University of Ha'il, Ha'il 55473, Saudi Arabia; hi.saber@uoh.edu.sa (H.S.); mo.abdelkader@uoh.edu.sa (A.M.)
[2] Department of Artificial Intelligence, College of Computer and Information Technology, Al-Razi University, Sana'a 12544, Yemen; dralmalahi@gmail.com
[3] Department of Mathematics, Hajjah University, Hajjah 00767, Yemen
[4] Technical and Engineering Unit, Applied College (Tanomah), King Khalid University, Abha 61413, Saudi Arabia; hamahmad@kku.edu.sa
[5] Department of Mathematics, Faculty of Science, Islamic University of Madinah, Madinah 42351, Saudi Arabia
[6] Department of Mathematics, Turabah University College, Taif University, Taif 21944, Saudi Arabia; al.amer@tu.edu.sa
[7] Department of Mathematics, University of Malakand, Chakdara 18000, Khyber Pakhtunkhwa, Pakistan; kamal@uom.edu.pk
* Correspondence: aldwoah@iu.edu.sa

Abstract: Many real-world phenomena exhibit multi-step behavior, demanding mathematical models capable of capturing complex interactions between distinct processes. While fractional-order models have been successfully applied to various systems, their inherent smoothness often limits their ability to accurately represent systems with discontinuous changes or abrupt transitions. This paper introduces a novel framework for analyzing nonlinear fractional evolution control systems using piecewise hybrid derivatives with respect to a nondecreasing function $\mathbb{W}(\iota)$. Building upon the theoretical foundations of piecewise hybrid derivatives, we establish sufficient conditions for the existence, uniqueness, and Hyers–Ulam stability of solutions, leveraging topological degree theory and functional analysis. Our results significantly improve upon existing theoretical understanding by providing less restrictive conditions for stability compared with standard fixed-point theorems. Furthermore, we demonstrate the applicability of our framework through a simulation of breast cancer disease dynamics, illustrating the impact of piecewise hybrid derivatives on the model's behavior and highlighting advantages over traditional modeling approaches that fail to capture the multi-step nature of the disease. This research provides robust modeling and analysis tools for systems exhibiting multi-step behavior across diverse fields, including engineering, physics, and biology.

Keywords: evolution control systems; topological degree theory; Lipchitz criteria; Hyers–Ulam stability; completely continuous; breast cancer model; simulation

Citation: Saber, H.; Almalahi, M.A.; Albala, H.; Aldwoah, K.; Alsulami, A.; Shah, K.; Moumen, A. Investigating a Nonlinear Fractional Evolution Control Model Using $\mathbb{W}$-Piecewise Hybrid Derivatives: An Application of a Breast Cancer Model. *Fractal Fract.* **2024**, *8*, 735. https://doi.org/10.3390/fractalfract8120735

Academic Editor: Corina S. Drapaca

Received: 30 October 2024
Revised: 5 December 2024
Accepted: 7 December 2024
Published: 13 December 2024

1. Introduction

Fractional calculus (FC) has emerged as a powerful tool for modeling complex phenomena across diverse fields [1–3]. However, traditional fractional derivatives [4–6], relying on a single memory kernel, are limited when modeling systems exhibiting multi-step behavior and crossover effects—where dominant factors shift over time. This limitation stems from their enforced uniform decay of past influences, failing to capture the varying dynamics often observed in real-world systems. Furthermore, existing analytical techniques, such as classical fixed-point theory, frequently impose restrictive conditions, hindering their

application to complex systems. To overcome these limitations, Atangana and Seda [7] introduced the piecewise hybrid fractional operator, which incorporates multiple fractional derivatives applied over distinct intervals. This innovative approach allows for a more nuanced representation of memory dynamics, as different derivatives can be tailored to specific phases, and the inclusion of transition points explicitly models crossover effects. This technique has already proven valuable in various applications, including modeling infectious diseases, biological interactions, and tumor growth [8–12]. Naik et al., in [8], developed an Ebola epidemic model incorporating a piecewise hybrid fractional operator and a Mittag-Leffler kernel to analyze disease dynamics and control factors. Alazman et al. in [9] analyzed a novel mathematical model using a system of differential equations with a piecewise fractional operator combining Caputo and Atangana–Baleanu derivatives. Saleem et al. [10] applied a classical piecewise hybrid model with a fractional derivative to an epidemic model. Aldowah et al. [11] presented numerical simulations of a piecewise dynamic model for malaria transmission. Sweilam et al. [12] presented a novel mathematical model of monkeypox disease dynamics with time delay, using a hybrid crossover approach and piecewise techniques. Some researchers have used piecewise hybrid fractional derivatives to analyze the dynamics of breast cancer at different disease stages (see [13–16]).

Lastly, to further enhance flexibility, enabling adaptation to diverse scenarios and datasets, in 2024, Alragad et al. [17] incorporated a variable memory kernel modulated by the nondecreasing function $\mathbb{W}(\iota)$. This function is important and plays a crucial role in enhancing the flexibility and adaptability of the piecewise hybrid fractional derivative approach. It essentially acts as a "time-warping" function, allowing the model to adapt to different time scales and incorporate variations in the rate of change in the system's dynamics. This approach is particularly crucial for modeling systems exhibiting complex, multi-step behavior and crossover effects. This novel approach shows promise for diverse applications. Alragad et al. [17] applied a ϕ-piecewise hybrid fractional derivative approach to investigate Ebola virus disease transmission dynamics. Sweilam et al. [18] presented a novel hybrid crossover model of monkeypox incorporating time delays. These advancements provide valuable insights into the complex dynamics of infectious diseases and improve our ability to predict and manage outbreaks. Their results have proven the importance of this technique in simulating the dynamics of the diseases transmission in its various stages well.

In this work, we incorporate a control variable function to investigate the nonlinear fractional evolution model by applying controllability criteria using the $\mathbb{W}$-piecewise hybrid derivative, incorporating a nondecreasing function $\mathbb{W}(\iota)$ that modulates the memory kernel, providing greater flexibility and adaptability for representing the varying influence of past events on a system's current state. This is particularly crucial for modeling systems exhibiting complex, multi-step behavior and crossover effects. This novel approach shows promise in diverse applications in different fields such as engineering, finance, environmental science, and biology. These advancements provide valuable insights into the complex dynamics of infectious diseases and improve our ability to predict and manage outbreaks. Using topological degree theory, we establish sufficient conditions for the existence, uniqueness, and Hyers–Ulam stability of solutions for nonlinear fractional evolution control systems employing the $\mathbb{W}$-piecewise hybrid derivative. Our framework addresses the limitations of traditional methods by providing a more robust and versatile tool for analyzing complex systems with dynamic memory characteristics. Specifically, our analysis overcomes the limitations of single fractional derivatives and simpler piecewise models by incorporating a variable memory kernel, modulated by $\mathbb{W}(\iota)$, providing a more realistic representation of systems where the influence of past events changes over time; it effectively captures multi-step behavior and crossover effects, avoiding the limitations of single fractional derivatives; it allows for a smooth transition between different dynamic regimes, unlike simpler piecewise models that often introduce discontinuities, and its flexibility and adaptability make it well suited to model diverse scenarios and datasets. The

choice of $\mathbb{W}(\iota)$ provides further control over the memory kernel to better reflect the specific dynamics of the system. We demonstrate the power of this new framework through its application to a breast cancer model to offer a significantly more nuanced representation of the disease's multi-stage progression. The variable memory kernel, modulated by $\mathbb{W}(\iota)$, allows for the accurate capture of the changing influence of past treatments, immune responses, and other factors on tumor growth. The ability to model crossover effects and smooth transitions between different disease stages enhances the model's biological realism and predictive power, leading to more effective strategies for understanding and treating breast cancer. Motivated by the importance of piecewise hybrid fractional derivative, we explore a category of fractional-order evolution control systems by applying controllability criteria. These systems are represented by the following equation, where $\iota \in J := [0, \chi]$,

$$\begin{cases} {}^{\mathbb{PCML}-\mathbb{W}(\iota)}_{0}\mathbf{D}_{\iota}^{\mathcal{Z}}\mathbb{K}(\iota) = \Phi\mathbb{K}(\iota) + \Psi\mathbb{V}(\iota) + \mathbb{F}(\iota, \mathbb{K}(\iota)), \\ \mathbb{K}(0) = \mathbb{K}_0, \end{cases} \tag{1}$$

where,

- Φ is the infinitesimal generator of an analytic semigroup of bounded linear operators on the Hilbert space $\mathbb{H}$.
- $\mathbb{V}$ is the control variable function on $L^2[J, \mathbb{H}]$ that represents the input to the system, allowing for manipulation of its trajectory.
- $\Psi : \mathbb{H} \to \mathbb{H}$ is a linear bounded operator that bridges the control input to the system's state, influencing how the control input affects the system's evolution.
- $\mathbb{F} : J \times \mathbb{R} \to \mathbb{R}$ represents potential nonlinearities in the system, adding complexity and potentially making the system more difficult to control.
- The increasing function $\mathbb{W}(\iota)$ plays a crucial role in enhancing the flexibility and adaptability of the $\mathbb{W}$-piecewise hybrid fractional derivative approach. It essentially acts as a "time-warping" function, allowing the model to adapt to different time scales and incorporate variations in the rate of change in the system's dynamics.
- $\mathbb{W}(\iota)$ can map the original time variable ι onto a new time scale, effectively stretching or compressing the time axis in different parts of the interval. This is particularly useful in modeling systems where the dynamics evolve at different rates in different phases. For example, in an infectious disease outbreak, the initial spread might be rapid, while the later stages might exhibit slower changes.

Nonlinear fractional evolution control systems (1), characterized by memory effects, nonlocal interactions, and complex dynamics, offer significant potential for modeling diverse real-world phenomena, including viscoelastic materials, financial markets, and biological systems exhibiting power-law behavior.

This research makes the following key contributions:

- A Novel Piecewise Hybrid Fractional Derivative Framework: We introduce a novel framework for modeling and analyzing nonlinear fractional evolution control systems using $\mathbb{PCML}$-$\mathbb{W}$ fractional derivatives. This approach overcomes limitations of both single fractional derivatives and simpler piecewise models by (a) employing a variable memory kernel (modulated by $\mathbb{W}(\iota)$) in the $\mathbb{W}$-$\mathbb{ML}$ component, thus providing a more realistic representation of systems where the influence of past events changes over time; and (b) enabling a smooth transition between distinct dynamic regimes (via a biologically relevant crossover point, ι_1) using the $\mathbb{W}$-Caputo and $\mathbb{W}$-$\mathbb{ML}$ components, thereby avoiding the artificial discontinuities of simpler piecewise methods.
- Robust Mathematical Framework: While classical fixed-point theory provides a useful tool for analyzing fractional differential equations (FDEs), its reliance on restrictive conditions, including strong compactness assumptions, limits its applicability. Coincidence degree methods [19–21] have expanded this scope, but limitations remain. Therefore, to analyze the broader class of nonlinear FDEs, particularly those involving piecewise fractional derivatives and control systems, we utilize the more versatile topological degree theory, which is capable of handling noncompact operators. Our

rigorous mathematical analysis, employing topological degree theory, establishes sufficient conditions for the existence, uniqueness, and Hyers–Ulam stability of solutions. This ensures the reliability and robustness of our model's predictions, even under small perturbations. Furthermore, we highlight the critical role of controllability analysis in developing effective control strategies.

- Controllability: This work highlights the critical role of controllability analysis in developing effective control strategies for these complex systems.
- Modeling Breast Cancer: We present a breast cancer model that uses $\mathbb{PCML}$-$\mathbb{W}$ fractional derivatives to accurately capture the transition from early-stage intrinsic growth to later stages. This transition is significantly influenced by treatment, immune response, and angiogenesis.

This piecewise hybrid derivative approach offers a more accurate, flexible, and biologically realistic framework than previous methods for modeling complex dynamical systems with multi-step behavior, demonstrating its significant advantage for applications, particularly in biological modeling.

2. Specific Techniques or Methods

This section lays the groundwork for our subsequent analysis by introducing key concepts related to the $\mathbb{PCML}$-$\mathbb{W}$ fractional derivative. In 2021, Atangana and Araz [7] explored new concepts in fractional derivatives, specifically piecewise hybrid fractional derivatives. One of these derivatives, called a piecewise hybrid derivative with Caputo and $\mathbb{ML}$ kernel, is defined as follows:

$$ {}^{\mathbb{PCML}}_{0}\mathbf{D}_{\iota}^{\mathcal{Z}}\mathbb{K}(\iota) = \begin{cases} {}^{\mathbb{C}}_{0}\mathbf{D}_{\iota}^{\mathcal{Z}}\mathbb{K}(\iota), & \iota \in [0, \iota_1], \\ {}^{\mathbb{ML}}_{0}\mathbf{D}_{\iota}^{\mathcal{Z}}\mathbb{K}(\iota), & \iota \in [\iota_1, \chi], \end{cases} $$

where the following hold:

- ${}^{\mathbb{C}}_{0}\mathbf{D}_{\iota}^{\mathcal{Z}}\mathbb{K}(\iota)$ represents the Caputo fractional derivative of order $\mathcal{Z}$,
- ${}^{\mathbb{ML}}_{0}\mathbf{D}_{\iota}^{\mathcal{Z}}\mathbb{K}(\iota) = {}^{\mathbb{ML}}\mathbf{D}_{0^+}^{\mathcal{Z}}\mathbb{K}(\iota) = \frac{\mathbb{ML}(\mathcal{Z})}{1-\mathcal{Z}}\int_0^{\iota} E_{\mathcal{Z}}\left(\frac{\mathcal{Z}}{\mathcal{Z}-1}(\iota-s)^{\mathcal{Z}}\right)\mathbb{K}'(s)ds$ represents the $\mathbb{ML}$ fractional derivative defined by Atangana and Baleanu [22].

The corresponding fractional integral ${}^{\mathbb{PCML}}_{0}\mathbf{I}_{\iota}^{\mathcal{Z}}$ is defined by

$$ {}^{\mathbb{PCML}}_{0}\mathbf{I}_{\iota}^{\mathcal{Z}}\mathbb{K}(\iota) = \begin{cases} {}^{\mathbb{RL}}_{0}\mathbf{I}_{\iota}^{\mathcal{Z}}\mathbb{K}(\iota), & \iota \in [0, \iota_1], \\ {}^{\mathbb{ML}}_{0}\mathbf{I}_{\iota}^{\mathcal{Z}}\mathbb{K}(\iota), & \iota \in [\iota_1, \chi], \end{cases} $$

where,

- ${}^{\mathbb{RL}}_{0}\mathbf{I}_{\iota}^{\mathcal{Z}}\mathbb{K}(\iota) = \frac{1}{\Gamma(\mathcal{Z})}\int_0^{\iota}(\iota-s)^{\mathcal{Z}-1}\mathbb{K}(s)ds$ represents the Riemann-Liouville fractional integral.
- ${}^{\mathbb{ML}}_{0}\mathbf{I}_{\iota}^{\mathcal{Z}}\mathbb{K}(\iota) = \frac{1-\mathcal{Z}}{\mathbb{ML}(\mathcal{Z})}\mathbb{K}(\iota) + \frac{\mathcal{Z}}{\mathbb{ML}(\mathcal{Z})\Gamma(\mathcal{Z})}\int_{\iota_1}^{\iota}(\iota-s)^{\mathcal{Z}-1}\mathbb{K}(s)ds$ represents the $\mathbb{ML}$ fractional integral.

In this work, building upon the definitions of the $\mathbb{ML}$-fractional derivative with respect to function $\mathbb{W}(\iota)$ [23] (denoted by $\mathbb{ML}-\mathbb{W}$) and the $\mathbb{C}$-fractional derivative with respect to function $\mathbb{W}(\iota)$ [24] (denoted by $\mathbb{C}-\mathbb{W}$), we present the definitions of piecewise hybrid derivative with a Caputo and $\mathbb{ML}$ kernel, with respect to function $\mathbb{W}(\iota)$ (denoted by $\mathbb{PCML}-\mathbb{W}(\iota)$), as follows:

$$ {}^{\mathbb{PCML}-\mathbb{W}(\iota)}_{0}\mathbf{D}_{\iota}^{\mathcal{Z}}\mathbb{K}(\iota) = \begin{cases} {}^{\mathbb{C}-\mathbb{W}(\iota)}_{0}\mathbf{D}_{\iota}^{\mathcal{Z}}\mathbb{K}(\iota), & \iota \in [0, \iota_1], \\ {}^{\mathbb{ML}-\mathbb{W}(\iota)}_{\iota_1}\mathbf{D}_{\iota}^{\mathcal{Z}}\mathbb{K}(\iota), & \iota \in [\iota_1, \chi], \end{cases} $$

where,

- ${}^{\mathbb{C}-\mathbb{W}(\iota)}_{0}\mathbf{D}^{\mathcal{Z}}_{\iota}\mathbb{K}(\iota)$ represents the Caputo fractional derivative with respect to function $\mathbb{W}(\iota)$,
- ${}^{\mathbb{ML}-\mathbb{W}(\iota)}_{\iota_1}\mathbf{D}^{\mathcal{Z}}_{\iota}\mathbb{K}(\iota) = \frac{\mathbb{ML}(\mathcal{Z})}{1-\mathcal{Z}}\int_0^{\iota}\mathbb{W}'(s)E_{\mathcal{Z}}\left(\frac{\mathcal{Z}(\mathbb{W}(\iota)-\mathbb{W}(s))}{\mathcal{Z}-1}\right)\mathbb{K}'_{\mathbb{W}}(s)ds$ represents the $\mathbb{ML}$ fractional derivative with respect to function $\mathbb{W}(\iota)$, where $\mathbb{W}'(\iota) \neq 0$ for all $\iota \in [0,\chi] \subset \mathbb{R}$, $\chi > 0$, and $\mathbb{K}'_{\mathbb{W}}(\iota) = \frac{\mathbb{K}'(\iota)}{\mathbb{W}'(\iota)}$, $\mathbb{W}'(\iota) \neq 0$, for all $\iota \in [0,\chi]$.

By allowing us to incorporate the influence of various factors affecting disease transmission, this generalization provides a more comprehensive and nuanced approach to modeling disease dynamics. The corresponding fractional integral is defined by

$${}^{\mathbb{PCML}-\mathbb{W}(\iota)}_{0}\mathbf{I}^{\mathcal{Z}}_{\iota}\mathbb{K}(\iota) = \begin{cases} {}^{\mathbb{C}-\mathbb{W}(\iota)}_{0}\mathbf{I}^{\mathcal{Z}}_{\iota}\mathbb{K}(\iota), & \iota \in [0,\iota_1], \\ {}^{\mathbb{ML}-\mathbb{W}(\iota)}_{0}\mathbf{I}^{\mathcal{Z}}_{\iota}\mathbb{K}(\iota), & \iota \in [\iota_1,\chi], \end{cases}$$

where,

- ${}^{\mathbb{C}-\mathbb{W}(\iota)}_{0}\mathbf{I}^{\mathcal{Z}}_{\iota}\mathbb{K}(\iota) = \frac{1}{\Gamma(\mathcal{Z})}\int_0^{\iota}\mathbb{X}^{\mathcal{Z}-1}_{\mathbb{W}}(\iota,s)\mathbb{K}(s)ds$ represents the Caputo fractional integral with respect to function $\mathbb{W}(\iota)$ [24].
- ${}^{\mathbb{ML}-\mathbb{W}(\iota)}_{0}\mathbf{I}^{\mathcal{Z}}_{\iota}\mathbb{K}(\iota) = \frac{1-\mathcal{Z}}{\mathbb{ML}(\mathcal{Z})}\mathbb{K}(\iota) + \frac{\mathcal{Z}}{\mathbb{ML}(\mathcal{Z})\Gamma(\mathcal{Z})}\int_{\iota_1}^{\iota}\mathbb{X}^{\mathcal{Z}-1}_{\mathbb{W}}(\iota,\sigma)\mathbb{K}(\sigma)d\sigma$ represents the $\mathbb{ML}$ fractional integral with respect to function $\mathbb{W}(\iota)$ [23],
- $\mathbb{X}^{\mathcal{Z}-1}_{\mathbb{W}}(\iota,s) = \mathbb{W}'(s)(\mathbb{W}(\iota)-\mathbb{W}(s))^{\mathcal{Z}-1}$.

To support our subsequent analysis, we utilize key findings from reference [25] regarding the properties and applications of topological degree theory.

Definition 1. *Let $\mathcal{N}$ be a Banach space of continuous functions on the interval $[0,\chi]$ equipped with the norm $\|\mathbb{K}\| = \max_{\iota\in[0,\chi]}|\mathbb{K}(\iota)|$. Let $\Delta \subset P(\mathcal{N})$ be the family of all bounded sets. The Kuratowski measure of noncompactness, $\xi(X)$, for a set $X \in \Delta$, is defined as*

$$\xi(X) = \inf\{r > 0 : X \text{ admits a finite cover by sets such } \psi(X) \leq r\},$$

where,

1. *$\psi(X)$ represents the diameter of X,*
2. *$\xi : \Delta \to \mathbb{R}_+$ represents the measure ξ.*

Definition 2. *Assume $\mathbb{G} : \Delta \subset \mathcal{N} \to \mathcal{N}$ is a continuous and bounded operator. Then, if*

$$\|\mathbb{G}(u) - \mathbb{G}(\widehat{u})\| \leq \Theta\|u - \widehat{u}\|, \Theta > 0,$$

for all $u, \widehat{u} \in \Delta$. Then, the operator $\mathbb{G}$ is Lipschitz with a specific constant Θ. Furthermore, if $\Theta < 1$, the operator $\mathbb{F}$ is classified as a strict contraction.

Proposition 1. *If $\mathbb{G} : \Delta \to \mathcal{N}$ is compact, then $\mathbb{G}$ satisfies the property of being Θ–Lipschitz with constants equal to 0.*

Definition 3 ([25])**.** *If $\mathbb{G} : \mathcal{N} \to \mathcal{N}$ is a Θ-condensing operator and*

$$D = \{\mathbb{K} \in \mathcal{N} : \exists \ell \in (0,1), \mathbb{K} = \ell\mathbb{G}(\mathbb{K})\}.$$

If $D \subset \mathcal{N}$ is bounded, and $D \subset \Omega_r(0)$, then

$$\deg(I - \ell\mathbb{G}, \Omega_r(0), 0) = 1, \text{ for all } \ell \in [0,1].$$

Consequently, the operator $\mathbb{G}$ possesses at least one fixed point, which is located within the ball $\Omega_r(0)$.

Lemma 1. *If* $\mathbb{K} \in H(0,\chi)$, $\mathbb{K} \in L(J)$, *the solution of*

$$\begin{cases} {}^{\mathbb{C}-\mathbb{W}(\iota)}_{0}\mathbf{D}_{\iota}^{\mathcal{Z}}\mathbb{K}(\iota) = \mathbb{K}(\iota), \\ \mathbb{K}(0) = \mathbb{K}_0, \end{cases}$$

is deduced as follows:

$$\mathbb{K}(\iota) = \mathbb{K}_0 + \frac{1}{\Gamma(\mathcal{Z})}\int_0^{\iota} \mathbb{X}_{\mathbb{W}}^{\mathcal{Z}-1}(\iota,\sigma)\mathbb{K}(\sigma)d\sigma.$$

Lemma 2. *If* $\mathbb{K} \in H(0,\chi)$, $\mathbb{K} \in L(J)$, *the solution of*

$$\begin{cases} {}^{\mathbb{ML}-\mathbb{W}(\iota)}_{0}\mathbf{D}_{\iota}^{\mathcal{Z}}\mathbb{K}(\iota) = \mathbb{K}(\iota), \\ \mathbb{K}(0) = \mathbb{K}_0, \end{cases}$$

is deduced as follows:

$$\mathbb{K}(\iota) = \mathbb{K}_{\iota_1} + \frac{1-\mathcal{Z}}{\mathbb{ML}(\mathcal{Z})}\mathbb{K}(\iota) + \frac{\mathcal{Z}}{\mathbb{ML}(\mathcal{Z})\Gamma(\mathcal{Z})}\int_{\iota_1}^{\iota} \mathbb{X}_{\mathbb{W}}^{\mathcal{Z}-1}(\iota,\sigma)\mathbb{K}(\sigma)d\sigma.$$

Theorem 1. *The solution of model (1) is given by*

$$\mathbb{K}(\iota) = \begin{cases} \mathbb{K}_0 + \frac{1}{\Gamma(\mathcal{Z})}\int_0^{\iota} \mathbb{X}_{\mathbb{W}}^{\mathcal{Z}-1}(\iota,\sigma)[\Phi\mathbb{K}(\sigma) + \Psi\mathbb{V}(\sigma) + \mathbb{F}(\sigma,\mathbb{K}(\sigma))]d\sigma, \\ \mathbb{K}_{\iota_1} + \frac{1-\mathcal{Z}}{\mathbb{ML}(\mathcal{Z})}[\Phi\mathbb{K}(\iota) + \Psi\mathbb{V}(\iota) + \mathbb{F}(\iota,\mathbb{K}(\iota))] \\ + \frac{\mathcal{Z}}{\mathbb{ML}(\mathcal{Z})\Gamma(\mathcal{Z})}\int_{\iota_1}^{\iota} \mathbb{X}_{\mathbb{W}}^{\mathcal{Z}-1}(\iota,\sigma)[\Phi\mathbb{K}(\sigma) + \Psi\mathbb{V}(\sigma) + \mathbb{F}(\sigma,\mathbb{K}(\sigma))]d\sigma. \end{cases}$$

Proof. By Lemmas 1 and 2 , the said solution can be obtained. □

Behavior of the System

To understand how the operators interact $\mathbb{W}$-Caputo and $\mathbb{W}-\mathbb{ML}$, and investigate the crossover point z_1 at which the dominant transmission mechanism shifts and to accurately represent the changing influence of various factors over time, we divide the study period $[0,\chi]$ into two sections: $[0,\iota_1]$ and $[\iota_1,\chi]$. This lets us see how the model's behavior shifts as we move from using the $\mathbb{W}$-Caputo derivative to the $\mathbb{W}-\mathbb{ML}$ derivative. Using this division, model (1) can be expressed as

$${}^{\mathbb{PCML}-\mathbb{W}(\iota)}_{0}\mathbf{D}_{\iota}^{\mathcal{Z}}\mathbb{K}(\iota) = \begin{cases} {}^{\mathbb{C}-\mathbb{W}(\iota)}_{0}\mathbf{D}_{\iota}^{\mathcal{Z}}\mathbb{K}(\iota) = \Phi\mathbb{K}(\iota) + \Psi\mathbb{V}(\iota) + \mathbb{F}(\iota,\mathbb{K}(\iota)), \iota \in [0,\iota_1], \\ {}^{\mathbb{ML}-\mathbb{W}(\iota)}_{\iota_1}\mathbf{D}_{\iota}^{\mathcal{Z}}\mathbb{K}(\iota) = \Phi\mathbb{K}(\iota) + \Psi\mathbb{V}(\iota) + \mathbb{F}(\iota,\mathbb{K}(\iota)), \iota \in [\iota_1,\chi], \end{cases}$$

where ${}^{\mathbb{C}-\mathbb{W}(\iota)}_{0}\mathbf{D}_{\iota}^{\mathcal{Z}}$ and ${}^{\mathbb{ML}-\mathbb{W}(\iota)}_{\iota_1}\mathbf{D}_{\iota}^{\mathcal{Z}}$ represent the Caputo and ML derivatives with respect to the function $\mathbb{W}(\iota)$, respectively. This division allows us to lead to a deeper understanding of the model's behavior and potential for improved accuracy and insights. In the following theorems, we analyze the properties of solutions of the system in both intervals and observe the impact of transitioning between different derivative operators.

3. Qualitative Analysis of the Model (1)

To discuss the qualitative analysis of Model (1), we use the topological degree theory. The following assumptions must be fulfilled for the analysis of the existence and uniqueness as well as stability results:

3.1. Hypothesis

(H_1) There exists a constant number $\mathbb{L}_{\mathbb{F}}0$ such that

$$\left|\mathbb{F}(\iota,\mathbb{K}(\iota))-\mathbb{F}\left(\iota,\widehat{\mathbb{K}}(\iota)\right)\right|\leq \mathbb{L}_{\mathbb{F}}\left|\mathbb{K}(\iota)-\widehat{\mathbb{K}}(\iota)\right|,\ \text{for}\ \iota\in\mathcal{J}\ \text{and}\ \mathbb{K},\widehat{\mathbb{K}}\in\mathcal{N}.$$

(H_2) $\mathbb{F}:\mathcal{J}\times\mathbb{R}\to\mathbb{R}$ is continuous, and there exist two constants $\tau_{\mathbb{F}},\eta_{\mathbb{F}}>0$ such that

$$|\mathbb{F}(\iota,\mathbb{K}(\iota))|\leq \tau_{\mathbb{F}}+|\mathbb{K}(\iota)|\eta_{\mathbb{F}},\ \text{for}\ \iota\in\mathcal{J}.$$

(H_3) For constants $\hbar_{\Phi},M_{\Psi}>0$, we have

$$|\Phi\mathbb{K}(\iota)|\leq \hbar_{\Phi}|\mathbb{K}(\iota)|,\qquad |\Psi\mathbb{V}(\sigma)|\leq M_{\Psi}.$$

3.2. Notations

In view of Theorem 1, we define an operator $\mathbb{G}:\mathcal{N}\to\mathcal{N}$ by

$$\mathbb{G}(\mathbb{K}(\iota))=\begin{cases}\mathbb{K}_0+\frac{1}{\Gamma(\mathcal{Z})}\int_0^{\iota}\mathbb{X}_{\mathbb{W}}^{\mathcal{Z}-1}(\iota,\sigma)[\Phi\mathbb{K}(\sigma)+\Psi\mathbb{V}(\sigma)+\mathbb{F}(\sigma,\mathbb{K}(\sigma))]d\sigma,\\ \mathbb{K}_{\iota_1}+\frac{1-\mathcal{Z}}{\mathbb{ML}(\mathcal{Z})}[\Phi\mathbb{K}(\iota)+\Psi\mathbb{V}(\iota)+\mathbb{F}(\iota,\mathbb{K}(\iota))]\\ +\frac{\mathcal{Z}}{\mathbb{ML}(\mathcal{Z})\Gamma(\mathcal{Z})}\int_{\iota_1}^{\iota}\mathbb{X}_{\mathbb{W}}^{\mathcal{Z}-1}(\iota,\sigma)[\Phi\mathbb{K}(\sigma)+\Psi\mathbb{V}(\sigma)+\mathbb{F}(\sigma,\mathbb{K}(\sigma))]d\sigma.\end{cases}\tag{2}$$

We observe that the model (1) has a solution if and only if the operator $\mathbb{G}$ possesses fixed points. Before we start our analysis, we use the following notations:

$$\begin{aligned}\mathcal{V}&=\max\left\{\frac{(\mathbb{W}(\iota_1)-\mathbb{W}(0))^{\mathcal{Z}}}{\Gamma(\mathcal{Z}+1)},\left(\frac{1-\mathcal{Z}}{\mathbb{ML}(\mathcal{Z})}+\frac{\mathcal{Z}(\mathbb{W}(\chi)-\mathbb{W}(\iota_1))^{\mathcal{Z}}}{\mathbb{ML}(\mathcal{Z})\Gamma(\mathcal{Z}+1)}\right)\right\},\\ \mathcal{O}&=\mathcal{V}(\hbar_{\Phi}+\eta_{\mathbb{F}}),\\ \Theta&=\mathcal{V}(\hbar_{\Phi}+\mathbb{L}_{\mathbb{F}}).\end{aligned}$$

3.3. Θ-Lipschitz

Lemma 3. *Under the assumption (H_1-H_3), the operator $\mathbb{G}$ is Θ-Lipschitz and satisfying the given condition*

$$\|\mathbb{G}(\mathbb{K})\|\leq[\max\{|\mathbb{K}_0|,|\mathbb{K}_{\iota_1}|\}+\mathcal{V}(M_{\Psi}+\tau_{\mathbb{F}})]+\mathcal{O}\|\mathbb{K}\|.$$

Proof. Let us take $\mathbb{K},\widehat{\mathbb{K}}\in\mathcal{N}$. Then, considering (2), for $\iota\in[0,\iota_1]$ we have

$$\left|\mathbb{G}(\mathbb{K}(\iota))-\mathbb{G}\left(\widehat{\mathbb{K}}(\iota)\right)\right|=\frac{1}{\Gamma(\mathcal{Z})}\int_0^{\iota}\mathbb{X}_{\mathbb{W}}^{\mathcal{Z}-1}(\iota,\sigma)\left[\Phi\left|\mathbb{K}(\sigma)-\widehat{\mathbb{K}}(\sigma)\right|+\left|\mathbb{F}(\sigma,\mathbb{K}(\sigma))-\mathbb{F}\left(\sigma,\widehat{\mathbb{K}}(\sigma)\right)\right|\right]d\sigma.$$

By (H_1) and (H_3), we have

$$\left|\mathbb{G}(\mathbb{K}(\iota))-\mathbb{G}\left(\widehat{\mathbb{K}}(\iota)\right)\right|\leq\frac{1}{\Gamma(\mathcal{Z})}\int_0^{\iota}\mathbb{X}_{\mathbb{W}}^{\mathcal{Z}-1}(\iota,\sigma)\left[\hbar_{\Phi}\left|\mathbb{K}(\sigma)-\widehat{\mathbb{K}}(\sigma)\right|+\mathbb{L}_{\mathbb{F}}\left|\mathbb{K}(\sigma)-\widehat{\mathbb{K}}(\sigma)\right|\right]d\sigma.$$

Hence,

$$\left\|\mathbb{G}(\mathbb{K})-\mathbb{G}\left(\widehat{\mathbb{K}}\right)\right\|\leq\frac{(\mathbb{W}(\iota_1)-\mathbb{W}(0))^{\mathcal{Z}}}{\Gamma(\mathcal{Z}+1)}\left[\hbar_{\Phi}\left\|\mathbb{K}-\widehat{\mathbb{K}}\right\|+\mathbb{L}_{\mathbb{F}}\left\|\mathbb{K}-\widehat{\mathbb{K}}\right\|\right].\tag{3}$$

For $\iota \in [\iota_1, \chi]$ we have

$$\begin{aligned} & \left|\mathbb{G}(\mathbb{K}(\iota)) - \mathbb{G}\left(\widehat{\mathbb{K}}(\iota)\right)\right| \\ \leq\ & \frac{1-\mathcal{Z}}{\mathbb{ML}(\mathcal{Z})}\left[\Phi\left|\mathbb{K}(\iota) - \widehat{\mathbb{K}}(\iota)\right| + \left|\mathbb{F}(\iota, \mathbb{K}(\iota)) - \mathbb{F}\left(\iota, \widehat{\mathbb{K}}(\iota)\right)\right|\right] \\ & + \frac{\mathcal{Z}}{\mathbb{ML}(\mathcal{Z})\Gamma(\mathcal{Z})}\int_{\iota_1}^{\iota} \mathbb{X}_{\mathbb{W}}^{\mathcal{Z}-1}(\iota, \sigma)\left[\Phi\left|\mathbb{K}(\sigma) - \widehat{\mathbb{K}}(\sigma)\right| + \left|\mathbb{F}(\sigma, \mathbb{K}(\sigma)) - \mathbb{F}\left(\sigma, \widehat{\mathbb{K}}(\sigma)\right)\right|\right] d\sigma. \end{aligned}$$

By (H_1) and (H_3), we have

$$\begin{aligned} & \left|\mathbb{G}(\mathbb{K}(\iota)) - \mathbb{G}\left(\widehat{\mathbb{K}}(\iota)\right)\right| \\ \leq\ & \frac{1-\mathcal{Z}}{\mathbb{ML}(\mathcal{Z})}\left[\hbar_{\Phi}\left|\mathbb{K}(\iota) - \widehat{\mathbb{K}}(\iota)\right| + \mathbb{L}_{\mathbb{F}}\left|\mathbb{K}(\iota) - \widehat{\mathbb{K}}(\iota)\right|\right] \\ & + \frac{\mathcal{Z}}{\mathbb{ML}(\mathcal{Z})\Gamma(\mathcal{Z})}\int_{\iota_1}^{\iota} \mathbb{X}_{\mathbb{W}}^{\mathcal{Z}-1}(\iota, \sigma)\left[\hbar_{\Phi}\left|\mathbb{K}(\sigma) - \widehat{\mathbb{K}}(\sigma)\right| + \mathbb{L}_{\mathbb{F}}\left|\mathbb{K}(\sigma) - \widehat{\mathbb{K}}(\sigma)\right|\right] d\sigma. \end{aligned}$$

Hence,

$$\left\|\mathbb{G}(\mathbb{K}) - \mathbb{G}\left(\widehat{\mathbb{K}}\right)\right\| \leq \left(\frac{1-\mathcal{Z}}{\mathbb{ML}(\mathcal{Z})} + \frac{\mathcal{Z}(\mathbb{W}(\chi) - \mathbb{W}(\iota_1))^{\mathcal{Z}}}{\mathbb{ML}(\mathcal{Z})\Gamma(\mathcal{Z}+1)}\right)\left[\hbar_{\Phi}\left\|\mathbb{K} - \widehat{\mathbb{K}}\right\| + \mathbb{L}_{\mathbb{F}}\left\|\mathbb{K} - \widehat{\mathbb{K}}\right\|\right]. \tag{4}$$

Then, by (3) and (4), we obtain

$$\left\|\mathbb{G}(\mathbb{K}) - \mathbb{G}\left(\widehat{\mathbb{K}}\right)\right\| \leq \Theta\left\|\mathbb{K} - \widehat{\mathbb{K}}\right\|.$$

Therefore, the operator $\mathbb{G}$ is Θ-Lipschitz. Furthermore, we can readily derive the growth condition as follows:

$$\|\mathbb{G}(\mathbb{K})\| \leq [\max\{|\mathbb{K}_0|, |\mathbb{K}_{\iota_1}|\} + \mathcal{V}(M_{\Psi} + \tau_{\mathbb{F}})] + \mathcal{O}\|\mathbb{K}\|.$$

□

3.4. Compactness of Operator $\mathbb{G}$

Lemma 4. *The operator $\mathbb{G} : \mathcal{N} \to \mathcal{N}$ is compact and, therefore, completely continuous.*

Proof. Define a bounded set $\Delta = \{\mathbb{K} \in \mathcal{N} : \|\mathbb{K}\| \leq r\}$ and consider sequences $\{\mathbb{K}_n\}, \{\mathbb{V}_n\}$ in Δ, such that $\mathbb{K}_n \to \mathbb{K}, \mathbb{V}_n \to \mathbb{V}$ as $n \to \infty$. Since Φ, Ψ and $\mathbb{F}$ are continuous mappings, we have

$$\begin{aligned} \Phi\mathbb{K}_n(\iota) &\to \Phi\mathbb{K}(\iota), \Psi\mathbb{V}_n(\iota) \to \Psi\mathbb{V}(\iota), \text{ as } n \to \infty, \\ \mathbb{F}(\iota, \mathbb{K}_n(\iota)) &\to \mathbb{F}(\iota, \mathbb{K}(\iota)), \text{ as } n \to \infty. \end{aligned}$$

Using H_1, we have

$$\begin{aligned} & \|\mathbb{G}(\mathbb{K}_n) - \mathbb{G}(\mathbb{K})\| \\ \leq\ & \begin{cases} \frac{(\mathbb{W}(\iota_1) - \mathbb{W}(0))^{\mathcal{Z}}}{\Gamma(\mathcal{Z}+1)}[(\hbar_{\Phi} + \mathbb{L}_{\mathbb{F}})\|\mathbb{K}_n - \mathbb{K}\|], \\ \left(\frac{1-\mathcal{Z}}{\mathbb{ML}(\mathcal{Z})} + \frac{\mathcal{Z}(\mathbb{W}(\chi) - \mathbb{W}(\iota_1))^{\mathcal{Z}}}{\mathbb{ML}(\mathcal{Z})\Gamma(\mathcal{Z}+1)}\right)[(\hbar_{\Phi} + \mathbb{L}_{\mathbb{F}})\|\mathbb{K}_n - \mathbb{K}\|], \end{cases} \\ \to\ & 0, \text{ as } n \to \infty. \end{aligned}$$

Thus, the operator $\mathbb{G}$ is continuous. By Lemma 3, we have

$$\|\mathbb{G}(\mathbb{K})\| \leq [\max\{|\mathbb{K}_0|, |\mathbb{K}_{\iota_1}|\} + \mathcal{V}(M_\Psi + \tau_\mathbb{F})] + \mathcal{O}r.$$

Hence, the operator $\mathbb{G}$ is bounded. For equicontinuity, let $0 < \iota_a < \iota_b < \iota_1, \mathbb{K} \in \Delta$. Then, we have

$$\begin{aligned}
& |\mathbb{G}(\mathbb{K}(\iota_b)) - \mathbb{G}(\mathbb{K}(\iota_a))| \\
= & \left| \frac{1}{\Gamma(\mathcal{Z})} \int_0^{\iota_b} \mathbb{X}_\mathbb{W}^{\mathcal{Z}-1}(\iota, \sigma)[\Phi\mathbb{K}(\sigma) + \Psi\mathbb{V}(\sigma) + \mathbb{F}(\sigma, \mathbb{K}(\sigma))]d\sigma \right. \\
& \left. - \frac{1}{\Gamma(\mathcal{Z})} \int_0^{\iota_a} \mathbb{X}_\mathbb{W}^{\mathcal{Z}-1}(\iota, \sigma)[\Phi\mathbb{K}(\sigma) + \Psi\mathbb{V}(\sigma) + \mathbb{F}(\sigma, \mathbb{K}(\sigma))]d\sigma \right| \\
\leq & \frac{1}{\Gamma(\mathcal{Z})} \int_0^{\iota_a} \mathbb{W}'(\sigma) \Big((\mathbb{W}(\iota_b) - \mathbb{W}(\sigma))^{\mathcal{Z}-1} - (\mathbb{W}(\iota_a) - \mathbb{W}(\sigma))^{\mathcal{Z}-1} \Big) \times \\
& [\Phi\mathbb{K}(\sigma) + \Psi\mathbb{V}(\sigma) + \mathbb{F}(\sigma, \mathbb{K}(\sigma))]d\sigma + \frac{1}{\Gamma(\mathcal{Z})} \int_{\iota_a}^{\iota_b} \mathbb{X}_\mathbb{W}^{\mathcal{Z}-1}(\iota, \sigma) \times \\
& [\Phi\mathbb{K}(\sigma) + \Psi\mathbb{V}(\sigma) + \mathbb{F}(\sigma, \mathbb{K}(\sigma))]d\sigma.
\end{aligned}$$

Thus, by (H_2), we have

$$\begin{aligned}
& \|\mathbb{G}(\mathbb{K}(\iota_b)) - \mathbb{G}(\mathbb{K}(\iota_a))\| \\
\leq & \frac{(\mathbb{W}(\iota_b) - \mathbb{W}(0))^{\mathcal{Z}} - (\mathbb{W}(\iota_a) - \mathbb{W}(0))^{\mathcal{Z}}}{\Gamma(\mathcal{Z}+1)} [\hbar_\Phi r + M_\Psi + \tau + r\eta].
\end{aligned}$$

Let $\iota_1 < \iota_a < \iota_b < \chi, \mathbb{K} \in \Delta$. Then, we have

$$\begin{aligned}
& |\mathbb{G}(\mathbb{K}(\iota_b)) - \mathbb{G}(\mathbb{K}(\iota_a))| \\
= & \left| \frac{1-\mathcal{Z}}{\mathbb{ML}(\mathcal{Z})} [\Phi\mathbb{K}(\iota_b) + \Psi\mathbb{V}(\iota_b) + \mathbb{F}(\iota_b, \mathbb{K}(\iota_b))] + \frac{\mathcal{Z}}{\mathbb{ML}(\mathcal{Z})\Gamma(\mathcal{Z})} \times \right. \\
& \int_{\iota_1}^{\iota_b} \mathbb{X}_\mathbb{W}^{\mathcal{Z}-1}(\iota_b, \sigma)[\Phi\mathbb{K}(\sigma) + \Psi\mathbb{V}(\sigma) + \mathbb{F}(\sigma, \mathbb{K}(\sigma))]d\sigma \\
& - \left[\frac{1-\mathcal{Z}}{\mathbb{ML}(\mathcal{Z})} [\Phi\mathbb{K}(\iota_a) + \Psi\mathbb{V}(\iota_a) + \mathbb{F}(\iota_a, \mathbb{K}(\iota_a))] + \frac{\mathcal{Z}}{\mathbb{ML}(\mathcal{Z})\Gamma(\mathcal{Z})} \times \right. \\
& \left. \left. \int_{\iota_1}^{\iota_a} \mathbb{X}_\mathbb{W}^{\mathcal{Z}-1}(\iota_a, \sigma) [\Phi\mathbb{K}(\sigma) + \Psi\mathbb{V}(\sigma) + \mathbb{F}(\sigma, \mathbb{K}(\sigma))]d\sigma \right] \right| \\
\leq & \frac{1-\mathcal{Z}}{\mathbb{ML}(\mathcal{Z})} ([\Phi\mathbb{K}(\iota_b) + \Psi\mathbb{V}(\iota_b) + \mathbb{F}(\iota_b, \mathbb{K}(\iota_b))] - [\Phi\mathbb{K}(\iota_a) + \Psi\mathbb{V}(\iota_a) + \mathbb{F}(\iota_a, \mathbb{K}(\iota_a))]) \\
& + \frac{\mathcal{Z}}{\mathbb{ML}(\mathcal{Z})\Gamma(\mathcal{Z})} \int_{\iota_1}^{\iota_a} \mathbb{W}'(\sigma) \Big((\mathbb{W}(\iota_b) - \mathbb{W}(\sigma))^{\mathcal{Z}-1} - (\mathbb{W}(\iota_a) - \mathbb{W}(\sigma))^{\mathcal{Z}-1} \Big) \times \\
& [\Phi\mathbb{K}(\sigma) + \Psi\mathbb{V}(\sigma) + \mathbb{F}(\sigma, \mathbb{K}(\sigma))]d\sigma + \frac{\mathcal{Z}}{\mathbb{ML}(\mathcal{Z})\Gamma(\mathcal{Z})} \int_{\iota_a}^{\iota_b} \mathbb{X}_\mathbb{W}^{\mathcal{Z}-1}(\iota, \sigma) \times \\
& [\Phi\mathbb{K}(\sigma) + \Psi\mathbb{V}(\sigma) + \mathbb{F}(\sigma, \mathbb{K}(\sigma))]d\sigma.
\end{aligned}$$

Thus, by (H_2), we have

$$\begin{aligned}
& \|\mathbb{G}(\mathbb{K}(\iota_b)) - \mathbb{G}(\mathbb{K}(\iota_a))\| \\
\leq & \frac{1-\mathcal{Z}}{\mathbb{ML}(\mathcal{Z})} ([\Phi\mathbb{K}(\iota_b) + \Psi\mathbb{V}(\iota_b) + \mathbb{F}(\iota_b, \mathbb{K}(\iota_b))] - [\Phi\mathbb{K}(\iota_a) + \Psi\mathbb{V}(\iota_a) + \mathbb{F}(\iota_a, \mathbb{K}(\iota_a))]) \\
& + \frac{\mathcal{Z}(\mathbb{W}(\iota_b) - \mathbb{W}(\iota_1))^{\mathcal{Z}} - (\mathbb{W}(\iota_a) - \mathbb{W}(\iota_1))^{\mathcal{Z}}}{\mathbb{ML}(\mathcal{Z})\Gamma(\mathcal{Z}+1)} [(\hbar_\Phi + \eta_\mathbb{F})r + M_\Psi + \tau_\mathbb{F}].
\end{aligned}$$

Moreover, utilizing the boundedness and continuity of $\mathbb{G}$, we have $\|\mathbb{G}(\mathbb{K}(\iota_b)) - \mathbb{G}(\mathbb{K}(\iota_a))\| \to 0$ as $\iota_a \to \iota_b$. This indicates that $\mathbb{G}$ is uniformly continuous. Consequently, by the Arzela–Ascoli theorem, we conclude that $\mathbb{G}$ is relatively compact and, therefore, completely continuous. □

3.5. Existence of Solution

Theorem 2. *The model (1) possesses a bounded set of solutions, guaranteeing the existence of at least one solution, provided that* $\mathcal{O} < 1$.

Proof. Based on Lemma 3, we conclude that the operator $\mathbb{G}$ is Θ-Lipschitz with a constant $\Theta \leq 1$. We can characterize a set of solutions for (1) as

$$D = \{\mathbb{K} \in \mathcal{N} : \exists \ell \in (0,1), \mathbb{K} = \ell \mathbb{G}(\mathbb{K})\},$$

which implies that

$$\begin{aligned} \|\mathbb{K}\| &= \|\ell \mathbb{G}(\mathbb{K})\| \\ &\leq \begin{cases} |\mathbb{K}_0| + \frac{(\mathbb{W}(\iota_1)-\mathbb{W}(0))^{\mathcal{Z}}}{\Gamma(\mathcal{Z}+1)}[(\hbar_\Phi + \eta_\mathbb{F})\|\mathbb{K}\| + M_\Psi + \tau_\mathbb{F}], \\ |\mathbb{K}_{\iota_1}| + \left(\frac{1-\mathcal{Z}}{\mathbb{ML}(\mathcal{Z})} + \frac{\mathcal{Z}(\mathbb{W}(\chi)-\mathbb{W}(\iota_1))^{\mathcal{Z}}}{\mathbb{ML}(\mathcal{Z})\Gamma(\mathcal{Z}+1)}\right)[(\hbar_\Phi + \eta_\mathbb{F})\|\mathbb{K}\| + M_\Psi + \tau_\mathbb{F}] \end{cases} \\ &\leq [\max\{|\mathbb{K}_0|, |\mathbb{K}_{\iota_1}|\} + \mathcal{V}(M_\Psi + \tau_\mathbb{F})] + \mathcal{O}\|\mathbb{K}\|. \end{aligned} \tag{5}$$

Let the set D be unbounded. By dividing both sides of (5) by $\|\mathbb{K}\|$, we obtain

$$1 \leq \lim_{\|\mathbb{K}\|\to\infty} \frac{1}{\|\mathbb{K}\|}([\max\{|\mathbb{K}_0|, |\mathbb{K}_{\iota_1}|\} + \mathcal{V}(M_\Psi + \tau_\mathbb{F})] + \mathcal{O}\|\mathbb{K}\|) \leq \mathcal{O} < 1.$$

This result is impossible, implying that the set D must be bounded. Therefore, $\mathbb{G}$ has at least one fixed point, which corresponds to a solution of the model (1). □

3.6. Uniqueness of Solution

Theorem 3. *Under assumptions* (H_1, H_3)*, the model (1) possesses a unique solution if* $\Theta < 1$.

Proof. By Lemma 3, we see that $\mathbb{G}$ is is Θ-Lipschitz. Thus, by the contraction mapping principle, we conclude that $\mathbb{G}$ has a unique fixed point, which corresponds to a unique solution of the model (1). □

3.7. Hyers–Ulam Stability

Hyers–Ulam stability is crucial in the study of functional equations as it provides a framework for understanding how small perturbations in inputs can affect outputs while ensuring the existence of nearby solutions. This concept is particularly important in applications across mathematics, physics, and engineering, where systems often experience minor deviations from ideal conditions. By establishing criteria for the stability of solutions, Hyers–Ulam stability aids in the analysis and control of dynamic systems, ensuring that approximate models can yield reliable predictions and behaviors [26]. Before presenting the crucial theorem regarding Hyers–Ulam stability for model (1), we introduce several definitions and an auxiliary Lemma to facilitate the discussion of the stability result.

Definition 4. *The model (1) is HU stable if there exists a real number* $\mathcal{M} > 0$ *such that for each* $\varepsilon > 0$*, there exists a unique solution* $\widehat{\mathbb{K}} \in \mathcal{N}$ *satisfies the following inequality:*

$$\left|{}_0^{\mathbb{PCML}-\mathbb{W}(\iota)}\mathbf{D}_\iota^{\mathcal{Z}}\widehat{\mathbb{K}}(\iota) - \left(\widehat{\mathbb{K}}(\iota) + \Psi\mathbb{V}(\iota) + \mathbb{F}\left(\iota, \widehat{\mathbb{K}}(\iota)\right)\right)\right| \leq \varepsilon, \iota \in \mathcal{J}, \tag{6}$$

corresponding to a solution $\mathbb{K} \in \mathcal{N}$ *of model (1) such that*

$$\left\| \widehat{\mathbb{K}} - \mathbb{K} \right\| \leq \mathcal{M}\varepsilon, \qquad \iota \in \mathcal{J},$$

Remark 1. *Let* Q *be a mapping in (*Q *dependent of* $\mathbb{K}$*), such that for any* $\varepsilon > 0$*:*
(i) $|Q(\iota)| \leq \varepsilon,\ \iota \in \mathcal{J}$*;*
(ii) The model (1) is considered as follows:

$$\begin{cases} {}_{0}^{\mathbb{PCML}-\mathbb{W}(\iota)}\mathbf{D}_{\iota}^{\mathcal{Z}}\mathbb{K}(\iota) = (\mathbb{K}(\iota) + \Psi\mathbb{V}(\iota) + \mathbb{F}(\iota, \mathbb{K}(\iota))) + Q(\iota), \\ \mathbb{K}(0) = \mathbb{K}_0. \end{cases} \tag{7}$$

The solution of (7) is given as follows:

$$\mathbb{K}(\iota) = \begin{cases} \mathbb{K}_0 + \frac{1}{\Gamma(\mathcal{Z})}\int_0^{\iota} \mathbb{X}_{\mathbb{W}}^{\mathcal{Z}-1}(\iota,\sigma)\times \\ [\Phi\mathbb{K}(\sigma) + \Psi\mathbb{V}(\sigma) + \mathbb{F}(\sigma, \mathbb{K}(\sigma))]d\sigma \\ + \frac{1}{\Gamma(\mathcal{Z})}\int_0^{\iota} \mathbb{X}_{\mathbb{W}}^{\mathcal{Z}-1}(\iota,\sigma)Q(\sigma)d\sigma, \\ \\ \mathbb{K}_{\iota_1} + \frac{1-\mathcal{Z}}{\mathbb{ML}(\mathcal{Z})}[\Phi\mathbb{K}(\iota) + \Psi\mathbb{V}(\iota) + \mathbb{F}(\iota, \mathbb{K}(\iota)) + Q(\iota)] \\ + \frac{\mathcal{Z}}{\mathbb{ML}(\mathcal{Z})\Gamma(\mathcal{Z})}\int_{\iota_1}^{\iota} \mathbb{X}_{\mathbb{W}}^{\mathcal{Z}-1}(\iota,\sigma)\times \\ [\Phi\mathbb{K}(\sigma) + \Psi\mathbb{V}(\sigma) + \mathbb{F}(\sigma, \mathbb{K}(\sigma))]d\sigma \\ + \frac{\mathcal{Z}}{\mathbb{ML}(\mathcal{Z})\Gamma(\mathcal{Z})}\int_{\iota_1}^{\iota} \mathbb{X}_{\mathbb{W}}^{\mathcal{Z}-1}(\iota,\sigma)Q(\sigma)d\sigma. \end{cases} \tag{8}$$

In view of Theorem 3, we may write (8) as follows in terms of the operator:

$$\mathbb{K}(\iota) = \mathbb{G}(\mathbb{K}(\iota)) + \begin{cases} \frac{1}{\Gamma(\mathcal{Z})}\int_0^{\iota} \mathbb{X}_{\mathbb{W}}^{\mathcal{Z}-1}(\iota,\sigma)Q(\sigma)d\sigma, \\ \\ \frac{1-\mathcal{Z}}{\mathbb{ML}(\mathcal{Z})}Q(\iota) + \frac{\mathcal{Z}}{\mathbb{ML}(\mathcal{Z})\Gamma(\mathcal{Z})}\int_{\iota_1}^{\iota} \mathbb{X}_{\mathbb{W}}^{\mathcal{Z}-1}(\iota,\sigma)Q(\sigma)d\sigma. \end{cases} \tag{9}$$

Lemma 5. *By the solution (9) and considering Remark 1 (i), we have*

$$|\mathbb{K}(\iota) - \mathbb{G}(\mathbb{K}(\iota))| \leq \max\left\{ \frac{(\mathbb{W}(\iota_1) - \mathbb{W}(0))^{\mathcal{Z}}}{\Gamma(\mathcal{Z}+1)}, \left(\frac{1-\mathcal{Z}}{\mathbb{ML}(\mathcal{Z})} + \frac{\mathcal{Z}(\mathbb{W}(\chi) - \mathbb{W}(\iota_1))^{\mathcal{Z}}}{\mathbb{ML}(\mathcal{Z})\Gamma(\mathcal{Z}+1)} \right) \right\}\varepsilon.$$

Proof. Consider the solution (9)

$$|\mathbb{K}(\iota) - \mathbb{G}(\mathbb{K}(\iota))| = \begin{cases} \left| \frac{1}{\Gamma(\mathcal{Z})}\int_0^{\iota} \mathbb{X}_{\mathbb{W}}^{\mathcal{Z}-1}(\iota,\sigma)Q(\sigma)d\sigma \right|, \\ \\ \left| \frac{1-\mathcal{Z}}{\mathbb{ML}(\mathcal{Z})}Q(\iota) + \frac{\mathcal{Z}}{\mathbb{ML}(\mathcal{Z})\Gamma(\mathcal{Z})}\int_{\iota_1}^{\iota} \mathbb{X}_{\mathbb{W}}^{\mathcal{Z}-1}(\iota,\sigma)Q(\sigma)d\sigma \right|. \end{cases} \tag{10}$$

Therefore, we have

$$\begin{aligned} |\mathbb{K}(\iota) - \mathbb{G}(\mathbb{K}(\iota))| &\leq \begin{cases} \frac{1}{\Gamma(\mathcal{Z})}\int_0^{\iota} \mathbb{X}_{\mathbb{W}}^{\mathcal{Z}-1}(\iota,\sigma)|Q(\sigma)|d\sigma, \\ \\ \frac{1-\mathcal{Z}}{\mathbb{ML}(\mathcal{Z})}|Q(\iota)| + \frac{\mathcal{Z}}{\mathbb{ML}(\mathcal{Z})\Gamma(\mathcal{Z})}\int_{\iota_1}^{\iota} \mathbb{X}_{\mathbb{W}}^{\mathcal{Z}-1}(\iota,\sigma)|Q(\sigma)|d\sigma \end{cases} \\ &\leq \begin{cases} \frac{(\mathbb{W}(\iota_1) - \mathbb{W}(0))^{\mathcal{Z}}}{\Gamma(\mathcal{Z}+1)}\varepsilon, \\ \\ \left(\frac{1-\mathcal{Z}}{\mathbb{ML}(\mathcal{Z})} + \frac{\mathcal{Z}(\mathbb{W}(\chi) - \mathbb{W}(\iota_1))^{\mathcal{Z}}}{\mathbb{ML}(\mathcal{Z})\Gamma(\mathcal{Z}+1)} \right)\varepsilon \end{cases} \\ &\leq \max\left\{ \frac{(\mathbb{W}(\iota_1) - \mathbb{W}(0))^{\mathcal{Z}}}{\Gamma(\mathcal{Z}+1)}, \left(\frac{1-\mathcal{Z}}{\mathbb{ML}(\mathcal{Z})} + \frac{\mathcal{Z}(\mathbb{W}(\chi) - \mathbb{W}(\iota_1))^{\mathcal{Z}}}{\mathbb{ML}(\mathcal{Z})\Gamma(\mathcal{Z}+1)} \right) \right\}\varepsilon. \end{aligned}$$

□

Theorem 4. *The solution of model (1) is Hyers–Ulam-stable and generalized-Hyers–Ulam-stable if* $\Theta < 1$.

Proof. Consider any solution $\mathbb{K}$ of model (1), and let $\widehat{\mathbb{K}}$ be the unique result, then we take

$$\begin{aligned}\left|\widehat{\mathbb{K}}(\iota) - \mathbb{K}(\iota)\right| &= \left|\widehat{\mathbb{K}}(\iota) - \mathbb{G}(\mathbb{K}(\iota))\right| \\ &= \left|\widehat{\mathbb{K}}(\iota) - \mathbb{G}\left(\widehat{\mathbb{K}}(\iota)\right) + \mathbb{G}\left(\widehat{\mathbb{K}}(\iota)\right) - \mathbb{G}(\mathbb{K}(\iota))\right| \\ &\leq \left|\widehat{\mathbb{K}}(\iota) - \mathbb{G}\left(\widehat{\mathbb{K}}(\iota)\right)\right| + \left|\mathbb{G}\left(\widehat{\mathbb{K}}(\iota)\right) - \mathbb{G}(\mathbb{K}(\iota))\right|.\end{aligned}$$

By Lemma 5 and Theorem 3, we have

$$\begin{aligned}\left|\widehat{\mathbb{K}}(\iota) - \mathbb{K}(\iota)\right| \leq\ & \max\left\{\frac{(\mathbb{W}(\iota_1) - \mathbb{W}(0))^{\mathcal{Z}}}{\Gamma(\mathcal{Z}+1)}, \left(\frac{1-\mathcal{Z}}{\mathbb{ML}(\mathcal{Z})} + \frac{\mathcal{Z}(\mathbb{W}(\chi) - \mathbb{W}(\iota_1))^{\mathcal{Z}}}{\mathbb{ML}(\mathcal{Z})\Gamma(\mathcal{Z}+1)}\right)\right\}\varepsilon \\ &+\Theta\left|\widehat{\mathbb{K}}(\iota) - \mathbb{K}(\iota)\right|,\end{aligned}$$

which further yields

$$\begin{aligned}\left\|\widehat{\mathbb{K}} - \mathbb{K}\right\| \leq\ & \max\left\{\frac{(\mathbb{W}(\iota_1) - \mathbb{W}(0))^{\mathcal{Z}}}{\Gamma(\mathcal{Z}+1)}, \left(\frac{1-\mathcal{Z}}{\mathbb{ML}(\mathcal{Z})} + \frac{\mathcal{Z}(\mathbb{W}(\chi) - \mathbb{W}(\iota_1))^{\mathcal{Z}}}{\mathbb{ML}(\mathcal{Z})\Gamma(\mathcal{Z}+1)}\right)\right\}\varepsilon \\ &+\Theta\left\|\widehat{\mathbb{K}} - \mathbb{K}\right\|.\end{aligned}$$

Thus, after simplification, we obtain

$$\left\|\widehat{\mathbb{K}} - \mathbb{K}\right\| \leq \frac{\max\left\{\frac{(\mathbb{W}(\iota_1) - \mathbb{W}(0))^{\mathcal{Z}}}{\Gamma(\mathcal{Z}+1)}, \left(\frac{1-\mathcal{Z}}{\mathbb{ML}(\mathcal{Z})} + \frac{\mathcal{Z}(\mathbb{W}(\chi) - \mathbb{W}(\iota_1))^{\mathcal{Z}}}{\mathbb{ML}(\mathcal{Z})\Gamma(\mathcal{Z}+1)}\right)\right\}}{1-\Theta}\varepsilon. \tag{11}$$

Hence, the solution of model (1) is Hyers–Ulam stable. Further, define a nondecreasing mapping $\Sigma : (0, \chi) \to \mathbb{R}$ as $\Sigma(\varepsilon) = \varepsilon$, such that $\Sigma(0) = 0$; then, from (11), one has

$$\left\|\widehat{\mathbb{K}} - \mathbb{K}\right\| \leq \frac{\max\left\{\frac{(\mathbb{W}(\iota_1) - \mathbb{W}(0))^{\mathcal{Z}}}{\Gamma(\mathcal{Z}+1)}, \left(\frac{1-\mathcal{Z}}{\mathbb{ML}(\mathcal{Z})} + \frac{\mathcal{Z}(\mathbb{W}(\chi) - \mathbb{W}(\iota_1))^{\mathcal{Z}}}{\mathbb{ML}(\mathcal{Z})\Gamma(\mathcal{Z}+1)}\right)\right\}}{1-\Theta}\Sigma(\varepsilon).$$

Therefore, the solution of model (1) is generalized-Hyers–Ulam-stable. □

The Hyers–Ulam stability bounds presented in Theorem 4 demonstrate the robustness of the model's solution to small perturbations. The Hyers–Ulam stability bound shows that the error between the exact solution and an approximate solution is directly proportional to the size of the perturbation ε. The generalized Hyers–Ulam stability bound, with a nondecreasing mapping $\Sigma(\varepsilon)$, where $\Sigma(0) = 0$, indicates that the error grows at a controlled rate as the perturbation increases. These bounds highlight the resilience of the system's behavior, even when confronted with uncertainties or errors in the model parameters or input, making it well suited for applications requiring reliable control and prediction. The magnitude of the bounds ($\mathcal{M}$ and $\Sigma(\varepsilon)$) directly reflects the robustness of the system, with smaller values indicating greater insensitivity to perturbations.

4. An Application

Breast cancer development is a nonuniform process, characterized by distinct stages with varying biological mechanisms. Early-stage tumor growth is primarily driven by intrinsic cellular processes, genetic mutations, and hormonal influences, often exhibiting

relatively rapid and exponential growth. A constant-memory kernel, such as that employed by the Caputo fractional derivative, effectively captures the dynamics of this initial phase, reflecting the cumulative impact of past genetic and environmental factors. However, later stages are significantly influenced by external factors including delayed treatment responses, dynamic immune system interactions, complex angiogenesis, and the potential for metastasis. These complexities necessitate a more adaptable model. The $\mathbb{W}-\mathbb{ML}$ fractional derivative, featuring a variable memory kernel modulated by the function $\mathbb{W}(\iota)$, is well suited for these later stages. $\mathbb{W}(\iota)$ allows for the accommodation of changes in the influence of past events due to treatment, immune responses, and other factors, capturing the dynamic memory inherent in these processes and the long-range interactions typical of complex biological systems. The crossover point, ι_1, between the $\mathbb{W}$-Caputo and $\mathbb{W}-\mathbb{ML}$ models represents a shift from predominantly intrinsic growth to a phase significantly influenced by external factors.

This piecewise approach, using the $\mathbb{PCML}-\mathbb{W}$ fractional derivative, effectively captures the dynamics of the breast cancer model across its different stages. The $\mathbb{PCML}-\mathbb{W}$ breast cancer model, a system of four coupled fractional differential equations, describes the populations of normal cells, tumor cells, immune response cells, and estrogen, incorporating control variables like anticancer drugs and ketogenic diet effects.

$$\begin{cases} {}_{0}^{\mathbb{PCML}-\mathbb{W}(\iota)}\mathbf{D}_{\iota}^{\mathcal{Z}}\mathbb{N}(\iota) = \mathbb{N}(\iota)m_1(A_1-\lambda_1\mathbb{N}(\iota)-\zeta_1\mathbb{T}(\iota))-(1-r)\mu_1\mathbb{N}(\iota)\mathbb{E}(\iota), \\ {}_{0}^{\mathbb{PCML}-\mathbb{W}(\iota)}\mathbf{D}_{\iota}^{\mathcal{Z}}\mathbb{T}(\iota) = \mathbb{T}(\iota)m_2(A_2-\lambda_3\mathbb{T}(\iota)-\zeta_2\mathbb{I}(\iota))+(1-r)\mu_1\mathbb{T}(\iota)\mathbb{N}(\iota)\mathbb{E}(\iota), \\ {}_{0}^{\mathbb{PCML}-\mathbb{W}(\iota)}\mathbf{D}_{\iota}^{\mathcal{Z}}\mathbb{I}(\iota) = \rho\gamma\mathbb{I}(\iota)+\mathbb{I}(\iota)(A_3-\lambda_5\mathbb{I}(\iota)-\zeta_3\mathbb{T}(\iota))-(1-r)\mu_2\mathbb{I}(\iota)\mathbb{E}(\iota), \\ {}_{0}^{\mathbb{PCML}-\mathbb{W}(\iota)}\mathbf{D}_{\iota}^{\mathcal{Z}}\mathbb{E}(\iota) = \mathbb{E}(\iota)((1-r)\alpha-\zeta_4\mathbb{E}(\iota)), \end{cases}$$

with the initial conditions

$$\mathbb{N}(0),\mathbb{T}(0),\mathbb{I}(0),\mathbb{E}(0)>0, \tag{12}$$

The population size is detailed in Table 1, while the model parameters and their estimates are outlined in Table 2.

Table 1. The population size for the breast cancer model.

Variable	Definition	Unit
$\mathbb{N}(\iota)$	This population represents healthy cells, with a growth rate of m_1 and a carrying capacity of A_1.	Cells
$\mathbb{T}(\iota)$	Malignant cancer cells, characterized by a growth rate of m_2 and a carrying capacity of A_2.	Cells
$\mathbb{I}(\iota)$	The body's defense against the tumor.	Cells
$\mathbb{E}(\iota)$	Level of estrogen in the body, which is produced at a source rate of α and eliminated at a rate of ζ_4.	ng/mL

Table 2. The descriptions and parameter values for the breast cancer model [27–29].

Parameter	Description	Value	Unit
m_1	Growth rate of normal cells	0.3	day^{-1}
A_1	Carrying capacity of normal cells	1.232	Cells
λ_1	Logistic rate for normal cell growth	0.1	day^{-1}
ζ_1	Inhibition rate of normal cells by tumor cells	6×10^{-8}	day^{-1}
μ_1	Rate of normal cell transformation to tumor cells	0.2	day^{-1}
r	Reduction factor for tumor cell formation due to anticancer drugs	0.5	
m_2	Growth rate of luminal-type tumor cells	0.4	day^{-1}
A_2	Carrying capacity of luminal-type tumor cells	2.35	Cells
λ_3	Logistic rate for luminal-type tumor cell growth	0.1	day^{-1}
ζ_2	Inhibition rate of luminal-type tumor cells by immune cells	3×10^{-6}	day^{-1}
ρ	Source rate of immune cells	130	day^{-1}
γ	Immune booster supplement (with $\rho \times \gamma = 1.3 \times 10^2$)	1	day^{-1}
A_3	Carrying capacity of immune cells	1.17	Cells
λ_5	Logistic rate for immune cell growth	0.1	day^{-1}
ζ_3	Inhibition rate of immune cells by tumor cells	1×10^{-7}	day^{-1}
μ_2	Suppression rate of immune cells by estrogen	0.002	day^{-1}
α	Source rate of estrogen	2	ng/mLday^{-1}
ζ_4	Elimination rate of estrogen	0.97	day^{-1}

This model describes the dynamics of four key cell populations in the context of breast cancer:

- The growth of normal cells $\mathbb{N}(\iota)$ is influenced by a logistic rate of (λ_1) and inhibited by tumor cells at a rate of (ζ_1). Tumor cells can evolve from normal cells at a rate of (μ_1), but this process is reduced by the effect of anticancer drugs, represented by $(1 - r)$.
- The growth of luminal-type tumor cells $\mathbb{T}(\iota)$ is influenced by a logistic rate of (λ_3) and inhibited by immune cells at a rate of (ζ_2). New tumor cell formation is promoted by estrogen $\mathbb{E}(\iota)$ at a rate represented by $\mu_1 \mathbb{N}(\iota)\mathbb{E}(\iota)$.
- Immune cells $\mathbb{I}(\iota)$ are continuously produced at a source rate ρ and the supplement of immune booster γ, with a carrying capacity of (A_3) and a logistic rate of (λ_5). Their growth is inhibited by tumor cells at a rate of (ζ_3) and suppressed by estrogen at a rate of (μ_2). Immune cell loss is also influenced by the combined effects of estrogen and anticancer drugs, as represented by $(1 - r)\mu_2 \mathbb{I}(\iota)\mathbb{E}(\iota)$.
- The level of estrogen $\mathbb{E}(\iota)$ in the body, which is produced at a source rate of (α) and eliminated at a rate of (ζ_4).

This model provides a framework for understanding the complex interactions between these populations and the potential influence of treatment interventions like anticancer drugs. The inclusion of fractional derivatives in the model allows for a more nuanced representation of memory effects and nonlocal interactions within the system.

Theorem 5. *The solution of* $(\mathbb{N}, \mathbb{T}, \mathbb{I}, \mathbb{E})$ *is positive with positive initial condition* $\mathbb{N}_0 > 0$, $\mathbb{T} > 0$, $\mathbb{I}_0 > 0$, $\mathbb{E}_0 > 0$.

Proof. Consider the above model, as follows:

$$\begin{cases} {}_{0}^{\mathbb{PCML}-\mathbb{W}(\iota)}\mathbf{D}_{\iota}^{\mathcal{Z}}\mathbb{N}(\iota)\Big|_{\mathbb{N}=0} = 0 \\ {}_{0}^{\mathbb{PCML}-\mathbb{W}(\iota)}\mathbf{D}_{\iota}^{\mathcal{Z}}\mathbb{N}(\iota)\Big|_{\mathbb{T}=0} = 0 \\ {}_{0}^{\mathbb{PCML}-\mathbb{W}(\iota)}\mathbf{D}_{\iota}^{\mathcal{Z}}\mathbb{N}(\iota)\Big|_{\mathbb{I}=0} = 0 \\ {}_{0}^{\mathbb{PCML}-\mathbb{W}(\iota)}\mathbf{D}_{\iota}^{\mathcal{Z}}\mathbb{N}(\iota)\Big|_{\mathbb{E}=0} = 0. \end{cases} \tag{13}$$

In view of Lemma 2, (13) yields that

$$\begin{aligned} \mathbb{N}(\iota) &= \mathbb{N}_0 > 0, \\ \mathbb{T}(\iota) &= \mathbb{T}_0 > 0, \\ \mathbb{I}(\iota) &= \mathbb{I}_0 > 0, \\ \mathbb{E}(\iota) &= \mathbb{E}_0 > 0, \end{aligned}$$

which implies that the solution

$$(\mathbb{N}(\iota), \mathbb{T}(\iota), \mathbb{I}(\iota), \mathbb{E}(\iota))$$

is positive for all $\iota > 0$. □

Theorem 6. *(Lipschitz property) Let* $\mathbb{N}, \mathbb{T}, \mathbb{I}, \mathbb{E}, \widehat{\mathbb{N}}, \widehat{\mathbb{T}}, \widehat{\mathbb{I}}, \widehat{\mathbb{E}}$, *be continuous functions in* $L^1[0,1]$. *Then, we obtain positive constants* c_1, c_2, c_3, *and* c_4 *such that*

$$\begin{aligned} \|\mathbb{N}\| &= \max_{\iota\in\mathcal{J}}|\mathbb{N}(\iota)| < c_1, \\ \|\mathbb{T}\| &= \max_{\iota\in\mathcal{J}}|\mathbb{T}(\iota)| < c_2, \\ \|\mathbb{I}\| &= \max_{\iota\in\mathcal{J}}|\mathbb{I}(\iota)| < c_3, \\ \|\mathbb{E}\| &= \max_{\iota\in\mathcal{J}}|\mathbb{E}(\iota)| < c_4, \end{aligned}$$

such that $\mathbb{F}_1, \mathbb{F}_2, \mathbb{F}_3, \mathbb{F}_4$ *defined by*

$$\begin{cases} \mathbb{F}_1(\iota, \mathbb{N}) = \mathbb{N}(\iota)m_1(A_1 - \lambda_1\mathbb{N}(\iota) - \zeta_1\mathbb{T}(\iota)) - (1-r)\mu_1\mathbb{N}(\iota)\mathbb{E}(\iota), \\ \mathbb{F}_1(\iota, \mathbb{T}) = \mathbb{T}(\iota)m_2(A_2 - \lambda_3\mathbb{T}(\iota) - \zeta_2\mathbb{I}(\iota)) + (1-r)\mu_1\mathbb{T}(\iota)\mathbb{N}(\iota)\mathbb{E}(\iota), \\ \mathbb{F}_1(\iota, \mathbb{I}) = \rho\gamma\mathbb{I}(\iota) + \mathbb{I}(\iota)(A_3 - \lambda_5\mathbb{I}(\iota) - \zeta_3\mathbb{T}(\iota)) - (1-r)\mu_2\mathbb{I}(\iota)\mathbb{E}(\iota), \\ \mathbb{F}_1(\iota, \mathbb{E}) = \mathbb{E}(\iota)((1-r)\alpha - \zeta_4\mathbb{E}(\iota)), \end{cases}$$

satisfy Lipschitz conditions with Lipschitz constant $\mathbb{L}_{\mathbb{F}} = \max_{i=1}^{4}\{\mathbb{L}_{\mathbb{F}_i}\} > 0$, *where*

$$\begin{aligned} \mathbb{L}_{\mathbb{F}_1} &= (m_1A_1 + m_1\lambda_1 + m_1\zeta_1c_2 + (1-r)\mu_1c_4), \\ \mathbb{L}_{\mathbb{F}_2} &= A_2m_2 + \lambda_3m_2 + m_2\zeta_2c_3 + (1-r)\mu_1c_1c_4, \\ \mathbb{L}_{\mathbb{F}_3} &= \rho\gamma + A_3 + \lambda_5 + \zeta_3c_2 + (1-r)\mu_2c_4, \\ \mathbb{L}_{\mathbb{F}_4} &= (1-r)\alpha - \zeta_4. \end{aligned}$$

Proof. Let $\mathbb{N}, \widehat{\mathbb{N}} \in L^1[0,1]$. Then,

$$\begin{aligned}\left\|\mathbb{F}_1(\iota,\mathbb{N})-\mathbb{F}_1\left(\iota,\widehat{\mathbb{N}}\right)\right\| &= \left\| \begin{array}{c} \mathbb{N}(\iota)m_1A_1-\mathbb{N}(\iota)m_1\lambda_1\mathbb{N}(\iota)-\mathbb{N}(\iota)m_1\zeta_1\mathbb{T}(\iota)-(1-r)\mu_1\mathbb{N}(\iota)\mathbb{E}(\iota) \\ -\left(\widehat{\mathbb{N}}(\iota)m_1A_1-\widehat{\mathbb{N}}(\iota)m_1\lambda_1\widehat{\mathbb{N}}(\iota)-\widehat{\mathbb{N}}(\iota)m_1\zeta_1\mathbb{T}(\iota)-(1-r)\mu_1\widehat{\mathbb{N}}(\iota)\mathbb{E}(\iota)\right) \end{array} \right\| \\ &\leq (m_1A_1+m_1\lambda_1+m_1\zeta_1c_2+(1-r)\mu_1c_4)\left\|\mathbb{N}-\widehat{\mathbb{N}}\right\|.\end{aligned}$$

Let $\mathbb{L}_{\mathbb{F}_1}=(m_1A_1+m_1\lambda_1+m_1\zeta_1c_2+(1-r)\mu_1c_4)>0$. Then, we have

$$\left\|\mathbb{F}_1(\iota,\mathbb{N})-\mathbb{F}_1\left(\iota,\widehat{\mathbb{N}}\right)\right\|\leq\mathbb{L}_{\mathbb{F}_1}\left\|\mathbb{N}-\widehat{\mathbb{N}}\right\|.$$

In the same manner, we can obtain the following:

$$\begin{aligned}\left\|\mathbb{F}_2(\iota,\mathbb{T})-\mathbb{F}_2\left(\iota,\widehat{\mathbb{T}}\right)\right\| &\leq \mathbb{L}_{\mathbb{F}_2}\left\|\mathbb{T}-\widehat{\mathbb{T}}\right\|, \\ \left\|\mathbb{F}_3(\iota,\mathbb{I})-\mathbb{F}_3\left(\iota,\widehat{\mathbb{I}}\right)\right\| &\leq \mathbb{L}_{\mathbb{F}_3}\left\|\mathbb{I}-\widehat{\mathbb{I}}\right\|,\end{aligned}$$

and

$$\left\|\mathbb{F}_4(\iota,\mathbb{E})-\mathbb{F}_4\left(\iota,\widehat{\mathbb{E}}\right)\right\|\leq\mathbb{L}_{\mathbb{F}_4}\left\|\mathbb{E}-\widehat{\mathbb{E}}\right\|.$$

Let

$$\mathbb{L}_{\mathbb{F}}=\max_{i=1}^{4}\{\mathbb{L}_{\mathbb{F}_i}\}>0.$$

Thus, $\mathbb{F}_i, i=1,2,3,4$ are Lipschitz continuous with a Lipschitz constant $\mathbb{L}_{\mathbb{F}}>0$. □

Matrix Form

Let us represent the given breast cancer model in the matrix form, taking into account the specific definitions and interpretations of each component:

- Define the State Vector $\mathbb{K}(\iota)$:

$$\mathbb{K}(\iota)=\begin{pmatrix}\mathbb{N}(\iota)\\ \mathbb{T}(\iota)\\ \mathbb{I}(\iota)\\ \mathbb{E}(\iota)\end{pmatrix}$$

  This vector represents the state of the system at time ι, capturing the populations of normal cells, tumor cells, immune response cells, and estrogen levels.
- Define the Control Variable Function $\mathbb{V}(\iota)$: Let us assume we have two control variables: $\mathbb{V}_1(\iota)$, which represents the effect of anticancer drugs.
  $\mathbb{V}_2(\iota)$, which represents the effect of a ketogenic diet. We can combine them into a vector:

$$\mathbb{V}(\iota)=\begin{pmatrix}\mathbb{V}_1(\iota)\\ \mathbb{V}_2(\iota)\end{pmatrix}$$

- Construct the Matrices: Φ: This matrix represents the linear dynamics of the system. We can derive it from the coefficients of the linear terms in the differential equations:

$$\Phi(\iota)=\begin{pmatrix}m_1A_1 & -m_1\zeta_1 & 0 & 0\\ 0 & m_2A_2-m_2\lambda_3 & -m_2\zeta_2 & 0\\ 0 & -\zeta_3 & \rho\gamma+A_3-\lambda_5 & 0\\ 0 & 0 & 0 & (1-r)\alpha\end{pmatrix}$$

- Construct the Matrices: Ψ: This matrix bridges the control input to the state. We need to determine how the control variables directly affect each population. Let us assume the following: $\mathbb{V}_1(\iota)$ (anticancer drugs) directly reduces tumor cell growth: Add a term $-d_1\mathbb{V}_1(\iota)$ to the second equation (tumor cell dynamics). $\mathbb{V}_2(\iota)$ (ketogenic diet) directly increases immune response cell population: Add a term $+d_2\mathbb{V}_2(\iota)$ to

the third equation (immune response cell dynamics). With these assumptions, the Ψ matrix becomes

$$\Psi(\iota) = \begin{pmatrix} 0 & 0 \\ -d_1 & 0 \\ 0 & d_2 \\ 0 & 0 \end{pmatrix}$$

where d_1 and d_2 are constants that represent the strength of the control variables' effects.

- $\mathbb{F}(\iota, \mathbb{K}(\iota))$: This vector represents the nonlinear terms in the system. We identify these from the following equations:

$$\mathbb{F}(\iota, \mathbb{K}(\iota)) = \begin{pmatrix} -m_1\lambda_1\mathbb{N}(\iota)^2 - (1-r)\mu_1\mathbb{N}(\iota)\mathbb{E}(\iota) \\ -m_2\lambda_3\mathbb{T}(\iota)^2 + (1-r)\mu_1\mathbb{T}(\iota)\mathbb{N}(\iota)\mathbb{E}(\iota) \\ -\lambda_5\mathbb{I}(\iota)^2 - (1-r)\mu_2\mathbb{I}(\iota)\mathbb{E}(\iota) \\ -\zeta_4\mathbb{E}(\iota)^2 \end{pmatrix}$$

- Initial Condition Vector $\mathbb{K}(0)$:

$$\mathbb{K}(0) = \begin{pmatrix} \mathbb{N}(0) \\ \mathbb{T}(0) \\ \mathbb{I}(0) \\ \mathbb{E}(0) \end{pmatrix}$$

- Final Matrix Representation: Now, we can express the model in the matrix form:

$$\begin{cases} {}^{\mathbb{PCML}-\mathbb{W}(\iota)}_{0}\mathbf{D}_{\iota}^{\mathcal{Z}}\mathbb{K}(\iota) = \Phi\mathbb{K}(\iota) + \Psi\mathbb{V}(\iota) + \mathbb{F}(\iota, \mathbb{K}(\iota)), \\ \mathbb{K}(0) = \mathbb{K}_0, \end{cases} \tag{14}$$

5. Numerical Scheme with $\mathbb{W}$-Piecewise Hybrid Derivative

To solve the fractional-order breast cancer model, we implement a numerical scheme leveraging the $\mathbb{W}$-piecewise hybrid fractional integral, specifically designed to handle the intricacies of this derivative type. The convergence and stability of a multi-step method like the one adopted depend on step size and other parameters. For instance, for a smooth problem with starting values up to $n-1$, the terms converge to the initial value of the problem as the step size is going to zero; then, in such case, the numerical solution converges to the exact one because the numerical solution of the proposed method depends on all the starting values of the numerical solution. Because any small perturbation produces a small effect in the solution, we say that the method is stable. Utilizing the $\mathbb{PCML}-\mathbb{W}$-fractional integral, we obtain the following numerical scheme:

$$\mathbb{N}(\iota) = \begin{cases} \mathbb{N}_0 + \frac{1}{\Gamma(\mathcal{Z})}\int_0^{\iota}\mathbb{X}_{\mathbb{W}}^{\mathcal{Z}-1}(\iota,\sigma)[\mathbb{N}m_1(A_1 - \lambda_1\mathbb{N} - \zeta_1\mathbb{T}) - (1-r)\mu_1\mathbb{NE}]d\sigma, \\ \mathbb{N}_{\iota_1} + \frac{1-\mathcal{Z}}{\mathbb{ML}(\mathcal{Z})}[\mathbb{N}m_1(A_1 - \lambda_1\mathbb{N} - \zeta_1\mathbb{T}) - (1-r)\mu_1\mathbb{NE}] \\ + \frac{\mathcal{Z}}{\mathbb{ML}(\mathcal{Z})\Gamma(\mathcal{Z})}\int_{\iota_1}^{\iota}\mathbb{X}_{\mathbb{W}}^{\mathcal{Z}-1}(\iota,\sigma)[\mathbb{N}m_1(A_1 - \lambda_1\mathbb{N} - \zeta_1\mathbb{T}) - (1-r)\mu_1\mathbb{NE}]d\sigma, \end{cases}$$

$$\mathbb{T}(\iota) = \begin{cases} \mathbb{T}_0 + \frac{1}{\Gamma(\mathcal{Z})}\int_0^{\iota}\mathbb{X}_{\mathbb{W}}^{\mathcal{Z}-1}(\iota,\sigma)[\mathbb{T}m_2(A_2 - \lambda_3\mathbb{T} - \zeta_2\mathbb{I}) + (1-r)\mu_1\mathbb{TNE}]d\sigma, \\ \mathbb{T}_{\iota_1} + \frac{1-\mathcal{Z}}{\mathbb{ML}(\mathcal{Z})}[\mathbb{T}m_2(A_2 - \lambda_3\mathbb{T} - \zeta_2\mathbb{I}) + (1-r)\mu_1\mathbb{TNE}] \\ + \frac{\mathcal{Z}}{\mathbb{ML}(\mathcal{Z})\Gamma(\mathcal{Z})}\int_{\iota_1}^{\iota}\mathbb{X}_{\mathbb{W}}^{\mathcal{Z}-1}(\iota,\sigma)[\mathbb{T}m_2(A_2 - \lambda_3\mathbb{T} - \zeta_2\mathbb{I}) + (1-r)\mu_1\mathbb{TNE}]d\sigma, \end{cases}$$

$$\mathbb{I}(\iota) = \begin{cases} \mathbb{I}_0 + \frac{1}{\Gamma(\mathcal{Z})}\int_0^{\iota}\mathbb{X}_{\mathbb{W}}^{\mathcal{Z}-1}(\iota,\sigma)[\rho\gamma\mathbb{I} + \mathbb{I}(A_3 - \lambda_5\mathbb{I} - \zeta_3\mathbb{T}) - (1-r)\mu_2\mathbb{IE}]d\sigma, \\ \mathbb{I}_{\iota_1} + \frac{1-\mathcal{Z}}{\mathbb{ML}(\mathcal{Z})}[\rho\gamma\mathbb{I} + \mathbb{I}(A_3 - \lambda_5\mathbb{I} - \zeta_3\mathbb{T}) - (1-r)\mu_2\mathbb{IE}] \\ + \frac{\mathcal{Z}}{\mathbb{ML}(\mathcal{Z})\Gamma(\mathcal{Z})}\int_{\iota_1}^{\iota}\mathbb{X}_{\mathbb{W}}^{\mathcal{Z}-1}(\iota,\sigma)[\rho\gamma\mathbb{I} + \mathbb{I}(A_3 - \lambda_5\mathbb{I} - \zeta_3\mathbb{T}) - (1-r)\mu_2\mathbb{IE}]d\sigma, \end{cases}$$

and

$$\mathbb{E}(\iota) = \begin{cases} \mathbb{E}_0 + \frac{1}{\Gamma(\mathcal{Z})}\int_0^{\iota} \mathbb{X}_{\mathbb{W}}^{\mathcal{Z}-1}(\iota,\sigma)[\mathbb{E}((1-r)\alpha - \zeta_4\mathbb{E})]d\sigma, \\ \mathbb{E}_{\iota_1} + \frac{1-\mathcal{Z}}{\mathbb{ML}(\mathcal{Z})}[\mathbb{E}((1-r)\alpha - \zeta_4\mathbb{E})] \\ + \frac{\mathcal{Z}}{\mathbb{ML}(\mathcal{Z})\Gamma(\mathcal{Z})}\int_{\iota_1}^{\iota} \mathbb{X}_{\mathbb{W}}^{\mathcal{Z}-1}(\iota,\sigma)[\mathbb{E}((1-r)\alpha - \zeta_4\mathbb{E})]d\sigma. \end{cases}$$

Now, put $\iota = \iota_{n+1}$, we obtain

$$\mathbb{N}(\iota_{n+1}) = \begin{cases} \mathbb{N}_0 + \frac{1}{\Gamma(\mathcal{Z})}\int_0^{\iota_{n+1}} \mathbb{X}_{\mathbb{W}}^{\mathcal{Z}-1}(\iota_{n+1},\sigma)[\mathbb{N}m_1(A_1 - \lambda_1\mathbb{N} - \zeta_1\mathbb{T}) - (1-r)\mu_1\mathbb{NE}]d\sigma, \\ \mathbb{N}_{\iota_1} + \frac{1-\mathcal{Z}}{\mathbb{ML}(\mathcal{Z})}[\mathbb{N}m_1(A_1 - \lambda_1\mathbb{N} - \zeta_1\mathbb{T}) - (1-r)\mu_1\mathbb{NE}] \\ + \frac{\mathcal{Z}}{\mathbb{ML}(\mathcal{Z})\Gamma(\mathcal{Z})}\int_{\iota_1}^{\iota_{n+1}} \mathbb{X}_{\mathbb{W}}^{\mathcal{Z}-1}(\iota_{n+1},\sigma)[\mathbb{N}m_1(A_1 - \lambda_1\mathbb{N} - \zeta_1\mathbb{T}) - (1-r)\mu_1\mathbb{NE}]d\sigma, \end{cases}$$

$$\mathbb{T}(\iota_{n+1}) = \begin{cases} \mathbb{T}_0 + \frac{1}{\Gamma(\mathcal{Z})}\int_0^{\iota_{n+1}} \mathbb{X}_{\mathbb{W}}^{\mathcal{Z}-1}(\iota_{n+1},\sigma)[\mathbb{T}m_2(A_2 - \lambda_3\mathbb{T} - \zeta_2\mathbb{I}) + (1-r)\mu_1\mathbb{TNE}]d\sigma, \\ \mathbb{T}_{\iota_1} + \frac{1-\mathcal{Z}}{\mathbb{ML}(\mathcal{Z})}[\mathbb{T}m_2(A_2 - \lambda_3\mathbb{T} - \zeta_2\mathbb{I}) + (1-r)\mu_1\mathbb{TNE}] \\ + \frac{\mathcal{Z}}{\mathbb{ML}(\mathcal{Z})\Gamma(\mathcal{Z})}\int_{\iota_1}^{\iota_{n+1}} \mathbb{X}_{\mathbb{W}}^{\mathcal{Z}-1}(\iota_{n+1},\sigma)[\mathbb{T}m_2(A_2 - \lambda_3\mathbb{T} - \zeta_2\mathbb{I}) + (1-r)\mu_1\mathbb{TNE}]d\sigma, \end{cases}$$

$$\mathbb{I}(\iota_{n+1}) = \begin{cases} \mathbb{I}_0 + \frac{1}{\Gamma(\mathcal{Z})}\int_0^{\iota_{n+1}} \mathbb{X}_{\mathbb{W}}^{\mathcal{Z}-1}(\iota_{n+1},\sigma)[\rho\gamma\mathbb{I} + \mathbb{I}(A_3 - \lambda_5\mathbb{I} - \zeta_3\mathbb{T}) - (1-r)\mu_2\mathbb{IE}]d\sigma, \\ \mathbb{I}_{\iota_1} + \frac{1-\mathcal{Z}}{\mathbb{ML}(\mathcal{Z})}[\rho\gamma\mathbb{I} + \mathbb{I}(A_3 - \lambda_5\mathbb{I} - \zeta_3\mathbb{T}) - (1-r)\mu_2\mathbb{IE}] \\ + \frac{\mathcal{Z}}{\mathbb{ML}(\mathcal{Z})\Gamma(\mathcal{Z})}\int_{\iota_1}^{\iota_{n+1}} \mathbb{X}_{\mathbb{W}}^{\mathcal{Z}-1}(\iota_{n+1},\sigma)[\rho\gamma\mathbb{I} + \mathbb{I}(A_3 - \lambda_5\mathbb{I} - \zeta_3\mathbb{T}) - (1-r)\mu_2\mathbb{IE}]d\sigma, \end{cases}$$

and

$$\mathbb{E}(\iota_{n+1}) = \begin{cases} \mathbb{E}_0 + \frac{1}{\Gamma(\mathcal{Z})}\int_0^{\iota_{n+1}} \mathbb{X}_{\mathbb{W}}^{\mathcal{Z}-1}(\iota_{n+1},\sigma)[\mathbb{E}((1-r)\alpha - \zeta_4\mathbb{E})]d\sigma, \\ \mathbb{E}_{\iota_1} + \frac{1-\mathcal{Z}}{\mathbb{ML}(\mathcal{Z})}[\mathbb{E}((1-r)\alpha - \zeta_4\mathbb{E})] \\ + \frac{\mathcal{Z}}{\mathbb{ML}(\mathcal{Z})\Gamma(\mathcal{Z})}\int_{\iota_1}^{\iota_{n+1}} \mathbb{X}_{\mathbb{W}}^{\mathcal{Z}-1}(\iota_{n+1},\sigma)[\mathbb{E}((1-r)\alpha - \zeta_4\mathbb{E})]d\sigma. \end{cases}$$

where

$$\mathbb{X}_{\mathbb{W}}^{\mathcal{Z}-1}(\iota,\sigma) = \mathbb{W}'(s)(\mathbb{W}(\iota) - \mathbb{W}(s))^{\mathcal{Z}-1}.$$

Convergence and Stability of the Numerical Scheme

Theorem 2 establishes sufficient conditions for the existence and uniqueness of a solution to the fractional-order breast cancer model, which is a prerequisite for the convergence of the numerical scheme. However, the convergence of the scheme itself is not directly established by Theorem 2 and requires a separate analysis. The convergence depends on several factors:

- The convergence of the numerical scheme depends on time step size. For small time step size, it shows divergence in the solution, but on large time step, we see the solutions of all classes tend to converge. Hence, we can say that the solution computed implies that a significant gain in efficiency can be achieved by step size control. This is not only for the computation of numerical solutions of ordinary deterministic differential equations but also for variable and fractional order problems. Also, the efficiency can be claimed for stochastic-type differential equations. Here, we used step size = 0.1 so that the solutions graphs of various compartments obtained show convergence behavior for almost all. If we increase the step size = 0.5, the graphs do not converge for all compartments. On checking it for step size = 0.01, we can also achieve the same results but the compilation time will increase as compared with using step size = 0.1. In the same way, by using step size = 0.01, we obtain stability in solution more rapidly as compared with step size = 0.1. Hence, the smallest values of perturbation in the initial condition if applied to obtain more stable results is 0.01. Here, we give the given Table 3. Here, it should be noted that the convergence

also depends on the value of variable-order and fractional-order values. For smooth variable orders and larger fractional orders, the convergence is faster. But stability in the case of the decay process is faster on smaller fractional orders, while in the growth process, it will be faster on larger fractional orders.

- The convergence of the numerical scheme depends on Lipschitz Continuity. Here, we noted that the nonlinear terms in the model satisfied a Lipschitz condition. See Theorem 6.

Table 3. CPU time for comparison for convergence and stability.

Step Size	CPU Time	Fractional Order $\mathcal{Z}$	$\mathbb{W}(\iota)$
0.01	2 s	0.75	ι
0.01	1.5 s	1.0	ι
0.1	1.2 s	0.75	ι
0.1	1 s	1.0	ι

6. Simulations and Discussion

Let us take the initial data $\mathbb{N}(0) = 200$, $\mathbb{T}(0) = 50$, $\mathbb{I}(0) = 50, \mathbb{E}(0) = 10$ and apply the numerical scheme established above to simulate our results graphically. Here, we presented the numerical illustrations for some different values of fractional order $\mathcal{Z}$ using $\mathbb{W}(\iota) = \iota$ in Figures 1–4, respectively.

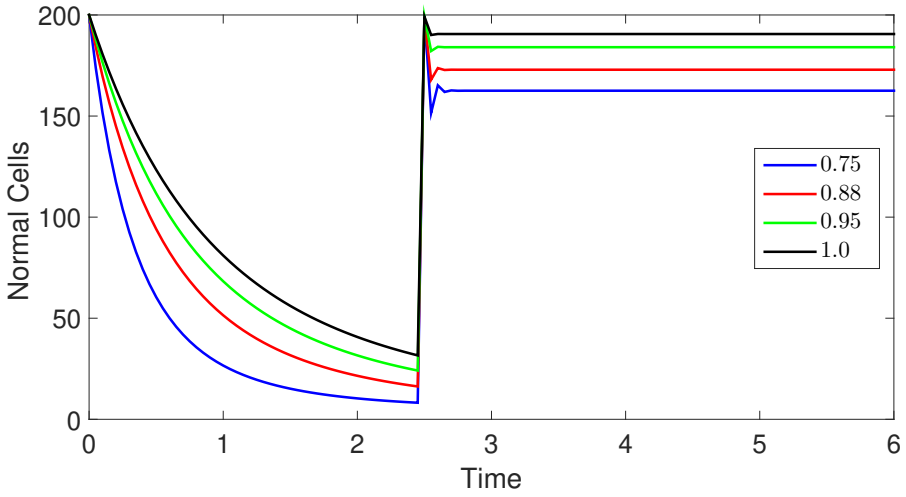

Figure 1. Numerical illustration for normal cell class of breast cancer model at fractional orders ranging from $\mathcal{Z} = 0.75$, $\mathcal{Z} = 0.88$, $\mathcal{Z} = 0.95$, to $\mathcal{Z} = 1.00$ with $\mathbb{W}(\iota) = \iota$.

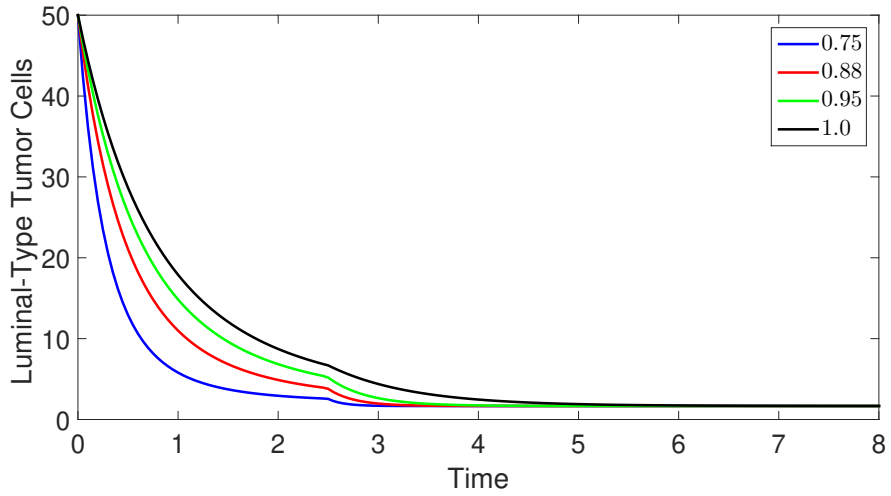

Figure 2. Numerical illustration for luminal-type tumor cell class of breast cancer model at fractional orders ranging from $\mathcal{Z} = 0.75$, $\mathcal{Z} = 0.88$, $\mathcal{Z} = 0.95$ to $\mathcal{Z} = 1.00$ with $\mathbb{W}(\iota) = \iota$.

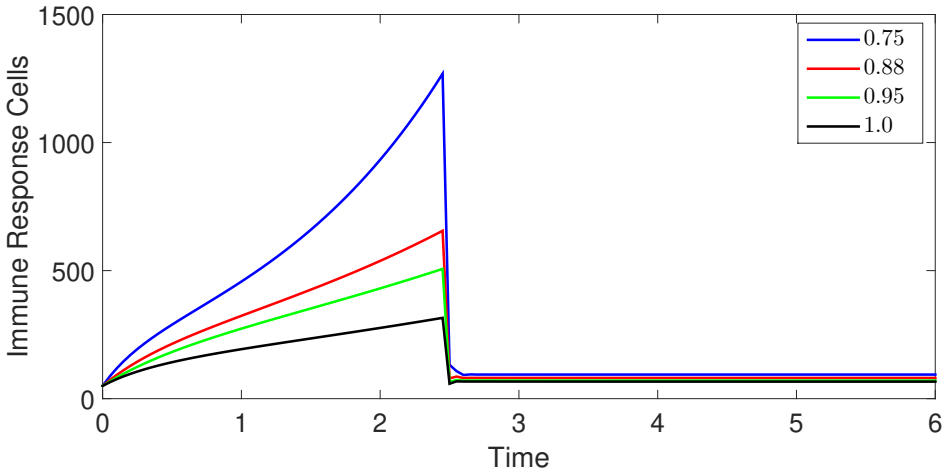

Figure 3. Numerical illustration for immune response cells class of breast cancer model at fractional orders ranging from $\mathcal{Z} = 0.75$, $\mathcal{Z} = 0.88$, $\mathcal{Z} = 0.95$ to $\mathcal{Z} = 1.00$ with $\mathbb{W}(\iota) = \iota$.

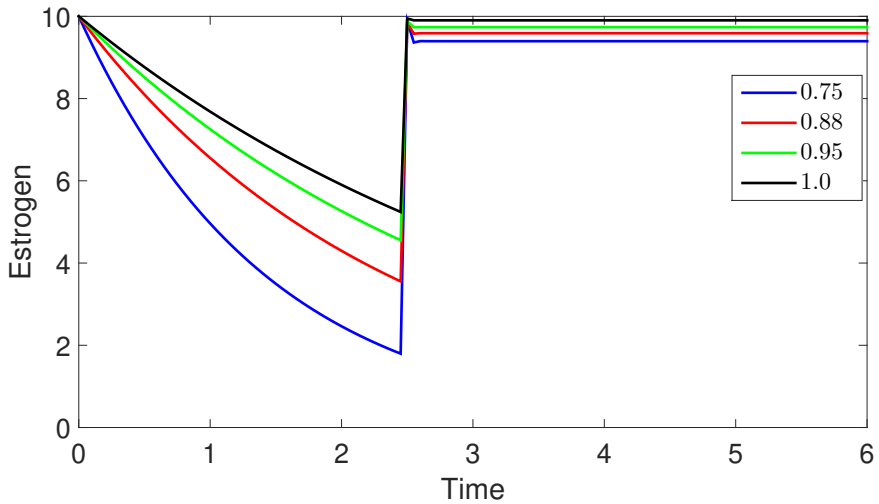

Figure 4. Numerical illustration for estrogen class of breast cancer model at fractional orders ranging from $\mathcal{Z} = 0.75$, $\mathcal{Z} = 0.88$, $\mathcal{Z} = 0.95$ to $\mathcal{Z} = 1.00$ with $\mathbb{W}(\iota) = \iota$.

The crossover behavior in each class can be seen for different fractional orders with the use of the given specific function $\mathbb{W}(\iota) = \iota$. We see that the population of normal cells first decreases and then becomes stable. In the same way, the population of luminal-type tumor cells decreases until it becomes stable. The number of immune response cells also rises, and then it falls. Further, the estrogen cells first decay and then rise.

The provided graphs illustrate the dynamics of four key cell populations in the context of breast cancer, simulated using a piecewise hybrid fractional derivative model. The model incorporates the effects of anticancer drugs and a ketogenic diet as control variables.

- Normal Cells: The graph shows that the normal cell population initially decreases rapidly, suggesting an initial rapid depletion of healthy cells, perhaps due to the onset of the disease or treatment. The population then stabilizes, indicating a balance between cell loss and regeneration.
- Luminal-Type Tumor Cells: The tumor cell population increases initially, reflecting tumor growth. The rate of increase gradually slows, potentially due to the combined effect of anticancer drugs and the immune response, which suppress tumor cell proliferation. The population eventually stabilizes at a higher level, suggesting that the treatment successfully controls tumor growth but does not eliminate it completely.
- Immune Response Cells: The immune response cells initially increase, indicating the activation of the immune system to fight the cancer. The population reaches a peak and then declines, possibly due to the depletion of immune cells as they combat the tumor.
- Estrogen: The estrogen level exhibits a sharp initial decrease, potentially due to the effects of treatment or disease progression on estrogen production or metabolism. After an initial decrease, the estrogen level stabilizes at a lower level, which might suggest a reduction in estrogen-driven tumor growth.

The Intersection Point: The point of intersection between the normal cell and tumor cell graphs represent a crucial threshold where the rate of normal cell loss is equal to the rate of tumor cell growth. This point marks a potential turning point in the disease trajectory, where the balance between healthy cells and tumor cells is shifting.

Importance of Piecewise Hybrid Fractional Derivative: the use of a piecewise hybrid fractional derivative offers several advantages over traditional fractional derivatives:

- Flexibility: The piecewise hybrid derivative allows for different fractional orders within different time intervals, accommodating the varying rates of change in complex biological systems. This is especially valuable in modeling disease progression, where different phases of the disease might involve different rates of cell growth, immune response, or estrogen production.
- Memory Effects: The piecewise hybrid derivative incorporates memory effects, allowing for the influence of past events on the current state [6,17]. In breast cancer, past treatments, diet, and other factors can influence the behavior of different cell populations over time. The piecewise approach allows for more realistic modeling of these memory effects.
- Crossover Effects: This approach captures the crossover effects, where the dominant factors influencing the system shift over time. For example, the effect of anticancer drugs might initially dominate, but as the tumor cells are suppressed, the immune system's role might become more prominent.

Overall, the graphs and analysis highlight the potential of piecewise hybrid fractional derivatives in modeling complex biological systems like breast cancer. The model captures the interplay of different cell populations, the effects of treatment, and the importance of memory and crossover effects. The point of intersection represents a significant threshold, where the balance between normal cells and tumor cells shifts, providing insights into the disease progression.

7. Conclusions

Nonlinear fractional evolution control systems are essential for modeling complex real-world phenomena exhibiting memory, nonlocal interactions, and complex dynamics—features poorly captured by linear models. Fractional derivatives account for memory effects, while nonlinearity reflects the often nonuniform and state-dependent nature of system interactions. This framework enables sophisticated control strategies with broad applications in biomedical systems (disease modeling, drug delivery), engineering, finance, and environmental science. This research contributes by investigating these systems using a novel piecewise hybrid derivative approach. We established sufficient conditions for the existence and uniqueness of solutions using topological degree theory and proved Hyers–Ulam stability, ensuring robustness to perturbations. This theoretical framework extends the capabilities of traditional fractional calculus to systems exhibiting multi-step behavior. The model successfully captures the transitions between different stages of disease progression by employing a $\mathbb{W}$-Caputo derivative for early stages and a $\mathbb{W} - \mathbb{ML}$ derivative for later stages. Numerical simulations, incorporating control variables (anticancer drugs and ketogenic diet), illustrate the model's ability to represent the dynamic interplay of cell populations and treatment responses. Our approach overcomes the limitations of previous studies using single fractional derivatives (with their constant memory kernels and inability to model multi-step behavior) and simpler piecewise models (characterized by arbitrary transition points, discontinuities, and limited memory flexibility) [15,16]. This piecewise hybrid model more accurately reflects the changing dynamics of breast cancer progression, with the transition point ι_1 representing a biologically significant shift from primarily intrinsic tumor growth to a phase dominated by external factors such as treatment and immune response. Future work will explore integrating this model with multi-scale modeling approaches to capture complex spatiotemporal interactions, enhancing its predictive capabilities.

Author Contributions: Conceptualization, M.A.A. and A.A.; Software, K.S.; Formal analysis, M.A.A. and A.A.; Investigation, A.A.; Writing—original draft, M.A.A.; Writing—review & editing, H.S., H.A., K.A. and A.M.; Project administration, K.A.; Funding acquisition, H.A. All authors have read and agreed to the published version of the manuscript.

Funding: This work was funded by Deanship of Research and Graduate Studies at King Khalid University through Small Group Research Project under grant number RGP1/21/45.

Data Availability Statement: Data are contained within the article.

Acknowledgments: The authors extend their appreciation to the Deanship of Research and Graduate Studies at King Khalid University for funding this work through Small Group Research Project under grant number RGP1/21/45.

Conflicts of Interest: The author declares that the research was conducted in the absence of any conflicts of interest.

References

1. Machado, J.T.; Kiryakova, V.; Mainardi, F. Recent history of fractional calculus. *Commun. Nonlinear Sci. Numer. Simul.* **2011**, *16*, 1140–1153. [CrossRef]
2. Meral, F.C.; Royston, T.J.; Magin, R. Fractional calculus in viscoelasticity: An experimental study. *Commun. Nonlinear Sci. Numer. Simul.* **2010**, *15*, 939–945. [CrossRef]
3. Kilbas, A.A.; Srivastava, H.M.; Trujillo, J.J. *Theory and Applications of Fractional Differential Equations*; North-Holland Mathematics Studies; Elsevier: New York, NY, USA; London, UK, 2006.
4. Samko, S.G.; Kilbas, A.A.; Marichev, O.I. *Fractional Integrals and Derivatives: Theory and Applications*; Gordon and Breach Science Publishers: Basel, Switzerland, 1993.
5. Podlubny, I. *Fractional Differential Equations*; Academic Press: San Diego, CA, USA, 1999.
6. Hamza, A.E.; Osman, O.; Ali, A.; Alsulami, A.; Aldwoah, K.; Mustafa, A.; Saber, H. Fractal-Fractional-Order Modeling of Liver Fibrosis Disease and Its Mathematical Results with Subinterval Transitions. *Fractal Fract.* **2024**, *8*, 638. [CrossRef]
7. Atangana, A.; Araz, S.I. New concept in calculus: Piecewise differential and integral operators. *Chaos Solitons Fractals* **2021**, *145*, 110638. [CrossRef]

8. Naik, P.A.; Farman, M.; Jamil, K.; Nisar, K.S.; Hashmi, M.A.; Huang, Z. Modeling and analysis using piecewise hybrid fractional operator in time scale measure for ebola virus epidemics under Mittag–Leffler kernel. *Sci. Rep.* **2024**, *14*, 24963. [CrossRef]
9. Alazman, I.; Alkahtani, B.S.T. Investigation of novel piecewise fractional mathematical model for COVID-19. *Fractal Fractional* **2022**, *6*, 661. [CrossRef]
10. Saleem, M.U.; Farman, M.; Nisar, K.S.; Ahmad, A.; Munir, Z.; Hincal, E. Investigation and application of a classical piecewise hybrid with a fractional derivative for the epidemic model: Dynamical transmission and modeling. *PLoS ONE* **2024**, *19*, e0307732. [CrossRef]
11. Aldwoah, K.A.; Almalahi, M.A.; Abdulwasaa, M.A.; Shah, K.; Kawale, S.V.; Awadalla, M.; Alahmadi, J. Mathematical analysis and numerical simulations of the piecewise dynamics model of Malaria transmission: A case study in Yemen. *AIMS Math.* **2024**, *9*, 4376–4408. [CrossRef]
12. Sweilam, N.H.; Al-Mekhlafi, S.M.; Hassan, S.M.; Alsenaideh, N.R.; Radwan, A.E. A Novel Hybrid Crossover Dynamics of Monkeypox Disease Mathematical Model with Time Delay: Numerical Treatments. *Fractal Fract.* **2024**, *8*, 185. [CrossRef]
13. Zanib, S.A.; Shah, M.A. A piecewise nonlinear fractional-order analysis of tumor dynamics: Estrogen effects and sensitivity. *Model. Earth Syst. Environ.* **2024**, *10*, 6155–6172. [CrossRef]
14. Deressa, C.T.; Mukharlyamov, R.G.; Nabwey, H.A.; Etemad, S.; Avci, I. On the Chaotic Nature of a Caputo Fractional Mathematical Model of Cancer and its Crossover Behaviors. *FRACTALS (Fractals)* **2024**, *32*, 1–21. [CrossRef]
15. Aldwoah, K.A.; Almalahi, M.A.; Hleili, M.; Alqarni, F.A.; Aly, E.S.; Shah, K. Analytical study of a modified-ABC fractional order breast cancer model. *J. Appl. Math. Comput.* **2024**, *70*, 3685–3716. [CrossRef]
16. Idrees, M.; Alnahdi, A.S.; Jeelani, M.B. Mathematical Modeling of Breast Cancer Based on the Caputo–Fabrizio Fractal-Fractional Derivative. *Fractal Fract.* **2023**, *7*, 805. [CrossRef]
17. Alraqad, T.; Almalahi, M.A.; Mohammed, N.; Alahmade, A.; Aldwoah, K.A.; Saber, H. Modeling Ebola Dynamics with a Φ-Piecewise Hybrid Fractional Derivative Approach. *Fractal Fract.* **2024**, *8*, 596. [CrossRef]
18. Sweilam, N.H.; Al-Mekhlafi, S.M.; Abdel Kareem, W.S.; Alqurishi, G. Comparative Study of Crossover Mathematical Model of Breast Cancer Based on ψ-Caputo Derivative and Mittag-Leffler Laws: Numerical Treatments. *Symmetry* **2024**, *16*, 1172. [CrossRef]
19. Ali, A.; Sarwar, M.; Zada, M.B.; Shah, K. Degree theory and existence of positive solutions to coupled system involving proportional delay with fractional integral boundary conditions. *Math. Methods Appl. Sci.* **2020**, *47*, 10582–10594.. [CrossRef]
20. Bohner, M.; Domoshnitsky, A.; Padhi, S.; Srivastava, S.N. Existence of solutions by coincidence degree theory for Hadamard fractionaldifferential equations at resonance. *Turk. J. Math.* **2024**, *48*, 296–306. [CrossRef]
21. Rezapour, S.; Thabet, S.T.; Rafeeq, A.S.; Kedim, I.; Vivas-Cortez, M.; Aghazadeh, N. Topology degree results on a G-ABC implicit fractional differential equation under three-point boundary conditions. *PLoS ONE* **2024**, *19*, e0300590. [CrossRef]
22. Atangana, A.; Baleanu, D. New fractional derivative with non-local and non-singular kernel. *Therm. Sci.* **2016**, *20*, 757–763. [CrossRef]
23. Fernandez, A.; Baleanu, D. Differintegration with respect to functions in fractional models involving Mittag-Leffler functions. In Proceedings of International Conference on Fractional Differentiation and Its Applications (ICFDA), Amman, Jordan, 16–18 July 2018.. [CrossRef]
24. Almeida, R. A Caputo fractional derivative of a function with respect to another function. *Commun. Nonlinear Sci. Numer. Simul.* **2017**, *44*, 460–481. [CrossRef]
25. Isaia, F. On a nonlinear integral equation without compactness. *Acta Math. Univ. Comen.* **2006**, *75*, 233–240.
26. Ibrahim, R.W. Generalized Hyers-Ulam stability for fractional differential equations. *Int. J. Math.* **2012**, *23*, 1250056. [CrossRef]
27. Oke, S.I.; Matadi, M.B.; Xulu, S.S. Optimal control analysis of a mathematical model for breast cancer. *Math. Comput. Appl.* **2018**, *23*, 21. [CrossRef]
28. Olufemi, A.S. Mathematical modelling of breast cancer thermo-therapy treatment: Ultrasound-based approach. *Math. Model.* **2016**, *2*, 1158–1164.
29. Isheden, G.; Humphreys, K. Modelling breast cancer tumour growth for a stable disease population. *Stat. Methods Med. Res.* **2019**, *28*, 681–702. [CrossRef]